

# Robustness of compositional heredity to the growth and division dynamics of prebiotic compartments

Yoshiya J. Matsubara,<sup>1,\*</sup> Sandeep Ameta,<sup>1</sup> Shashi Thutupalli,<sup>1,2</sup> Philippe Nghe,<sup>3</sup> and Sandeep Krishna<sup>1</sup>

<sup>1</sup>*Simons Centre for the Study of Living Machines, National Centre for Biological Sciences, Tata Institute of Fundamental Research, Bengaluru, India*

<sup>2</sup>*International Centre for Theoretical Sciences, Tata Institute of Fundamental Research, Bengaluru, India*

<sup>3</sup>*Laboratory of Biophysics and Evolution, UMR CNRS-ESPCI Chemistry Biology Innovation, École Supérieure de Physique et de Chimie Industrielles de la Ville de Paris (ESPCI Paris), PSL University, France*

(Dated: November 8, 2022)

An important transition after the origin of life was the first emergence of a Darwinian population, self-reproducing entities exhibiting differential reproduction, phenotypic variation, and inheritance of phenotypic traits. The simplest system we can imagine to have these properties would consist of a compartmentalized autocatalytic reaction system that exhibits two growth states with different chemical compositions. Identifying the chemical composition as the phenotype, this accounts for two of the properties. However, it is not clear what are the necessary conditions for such a chemical system to exhibit inheritance of the compositional states upon growth and division of the compartment. We show that for a general class of autocatalytic chemical systems subject to serial dilution, the inheritance of compositional information only occurs when the time interval between dilutions is below a critical threshold that depends on the efficiency of the catalytic reactions. Further, we show that these thresholds provide rigorous bounds on the properties required for the inheritance of the chemical compositional state for general growth and division cycles. Our result suggests that a serial dilution experiment, which is much easier to set up in a laboratory, can be used to test whether a given autocatalytic chemical system can exhibit heredity. Lastly, we apply our results to a realistic autocatalytic system based on the *Azoarcus* ribozyme and suggest a protocol to experimentally test whether this system can exhibit heredity.

Keywords: bistability, autocatalytic sets, compartmentalization, growth and division, Darwinian evolution, heredity, serial dilution, continuous stirred-tank reactor

## I. INTRODUCTION

The origin of life on Earth involved the transition from a primordial “soup” of chemicals to a population of self-reproducing individuals evolving under natural selection. There have been a number of proposals for the nature of the earliest self-reproducing entities, ranging from RNA [1, 2] to clay [3] to X. Even within broadly supported frameworks like the RNA world [4], there are many possibilities – some have advocated for collective autocatalytic sets [5–8] while others search for the simplest RNA ribozyme that can copy itself [9]. There are also multiple proposals for a compartment that separates a self-reproducing individual from its environment and other individuals [10], ranging from lipid membranes [11] to coacervates [12] to spatial separation on surfaces [13, 14], or within hydrodynamic flows [15]. Regardless of the details, one could describe the emergent population as consisting of autocatalytic chemical entities confined within compartments that grow and divide to produce new offspring individuals. We use “autocatalytic chemical entities” and “compartments” very broadly to encompass all the possibilities described above. For such a system to be considered a population evolving under natural selection [16], it must have certain

properties. Following Godfrey-Smith [17], who analyzes and builds on formulations by Lewontin [18], Endler [19], Ridley [20], and others, we expect the individuals to exhibit:

1. Phenotypic variation
2. Differential reproduction
3. Inheritance of phenotypic traits (“heredity”)

We ask: if one is provided an autocatalytic chemical system that could be confined to compartments that grow and divide as the system consumes food molecules to self-reproduce from the environment, how can one test whether it has all the above properties? One of the simplest dynamical (chemical) systems that have the properties enumerated by Godfrey-Smith consists of a bistable chemical system, which exhibits two growth states with different chemical compositions and, in general, different growth rates. We define a growth state as one where the concentrations of the chemicals comprising the system grow without bound (often exponentially) as the system consumes food molecules, but where the chemical composition – the relative concentrations of the chemical components – reaches a steady state. Identifying the chemical composition to be the individual’s phenotype accounts for phenotypic variation, and assuming the chemical composition affects the growth and division process accounts for differential reproduction [21]. In the

---

\* yoshiyam@ncbs.res.in

language of dynamical systems, the third property of inheritance translates to the stability of the two growth states (hence our term ‘bistable chemical system’) (see Fig. 1). Here, by stability, we mean that the system does not spontaneously transition from one growth state to the other *when it divides into two offspring entities* [22].

The inheritance of the compositional information has been previously debated in a number of models of autocatalytic networks [23–27]. One suggestion has been that the network must contain multiple ‘viable autocatalytic cores’ [25, 28] in order to exhibit heredity. Another suggestion is that the chemical system could show multiple compositional states as the response to environmental changes (e.g., change of the food set molecules) [29–31]. However, it is unclear whether such mechanisms could be stable enough to stochastic noise or environmental fluctuations, let alone to the growth and division dynamics of compartments, which would be needed for the inheritance of information across generations.

Multistability in chemical systems has been extensively studied in the context of epigenetic memory in gene regulatory networks [32], signaling pathways [33], metabolic networks [34], chiral symmetry breaking [35, 36], or enzymatic cascades [37–41], etc. Generally speaking, positive feedback in the network structure is necessary though not sufficient for multistability [42], and more detailed conditions have also been suggested in specific contexts [43] [44]. However, these conditions for bi/multistability have been investigated mainly in chemostat or continuously-stirred-tank-reactor (CSTR) scenarios where there is a constant influx and outflux [45]. It has not systematically been investigated under the conditions where these reaction systems are enclosed within a compartment that dynamically grows and divides.

Thus, our question narrows to: if one is provided an autocatalytic chemical system capable of exhibiting two distinct growth states, what are the necessary conditions to ensure that these states will be stable upon growth and division of the compartments that enclose these entities? We study this question theoretically using deterministic dynamical models of a class of autocatalytic chemical systems that exhibit two exponential growth states. We analyze the stability of these states when subjected to the additional growth and division process. We first show that the dynamics of a general growth and division process can range from a chemostat-like (CSTR) condition, where the rate equations are subject to influx and outflux of molecules at a constant rate, to sudden periodic reductions of the chemical concentrations. A formulation that models growth and division as a serial dilution protocol [46] captures these extremes and everything in between. We find the inheritance of the compositional state under serial dilution only when the time interval between dilutions is below a critical threshold that depends on the efficiency of the catalytic reactions. A similar critical threshold is found for the average dilution rate. These thresholds provide bounds on the properties of general growth and division cycles which, if violated, will de-

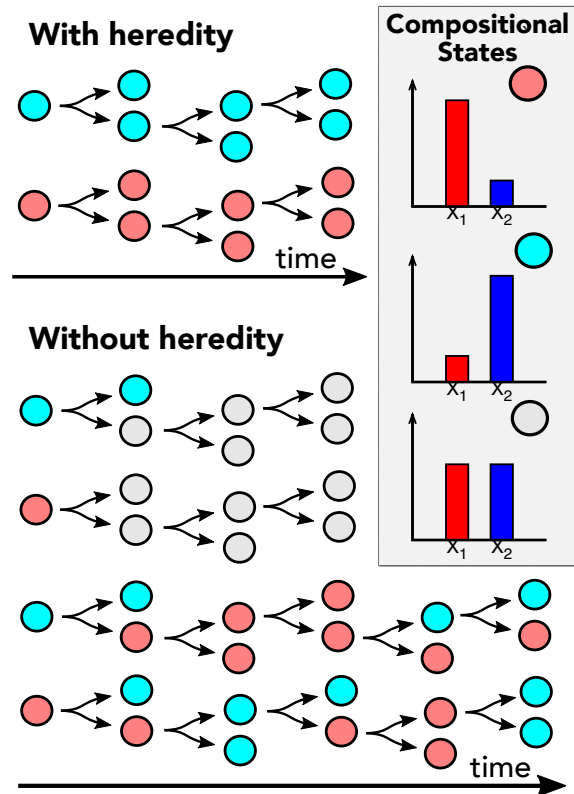


FIG. 1. A sketch of the schematic figures for explaining compartments with and without heredity. Red, blue, and grey circles represent variations of reproducing compartments with different compositions within them under the same environment. (Top) reproduction of compartments with heredity: daughters have the same composition as their parents. (Bottom) Heredity can break down in two ways: either, the chemical composition converges to the same single grey state irrespective of the initial state, or spontaneous transitions between the two growth states, red and blue, are so rapid that all information about the initial state is lost very quickly.

stroy the heredity of the chemical compositional state. Moreover, because serial dilution is a protocol much more easily implemented in the laboratory than the growth and division of compartments, this provides a relatively easy experimental test for whether a given autocatalytic chemical system is capable of exhibiting heredity. We illustrate our results with models of a realistic instance of such an autocatalytic chemical system, based on a ribozyme from the *Azoarcus* bacterium engineered to self-reproduce from smaller their fragments [30, 47, 48].

## II. RESULTS

### A. Mapping general growth and division scenarios to the serial dilution protocol

First, we discuss how compartments’ growth and division (GD) affect the chemical reaction systems encapsu-

lated within them. As compartments grow and divide, the chemical concentrations within them change due to the chemical reactions occurring, but also get diluted due to increases in the compartment volume. If the compartment volume grows between division as  $V(t)$ , then the dilution rate is  $\phi(t) \equiv \frac{dV}{dt}(t)/V(t)$ . An influx of substrates from outside the compartment may also occur, increasing the amount of those components. Thus, the chemical rate equations must include terms for such influx and dilution. Initially, we consider three assumptions on such a GD process, some of which will be relaxed in later sections:

1. Compartments divide into  $m$  equal-sized smaller ones periodically, at time intervals of  $\Delta t$  (see Fig. 2A).
2. We assume a well-mixed condition inside a compartment. This implies that the *concentrations* do not change at divisions because the chemical components are partitioned proportionally to the volumes of the daughter compartments.
3. For simplicity, we assume the influx rate of substrates  $\sigma(t)$  is proportional to the dilution rate  $\phi(t)$  (this is not an important assumption; if  $\sigma(t)$  is an arbitrary function with periodicity  $\Delta t$  our results do not qualitatively change).

Typical dilution protocols that are used in laboratories, such as serial dilution (SD) or the continuous stirred-tank reactor (CSTR), are special cases of the compartment GD scenario: If  $\phi(t)$  (and  $\sigma(t)$ ) have sharp spikes at times  $t = n\Delta t$  ( $n = 1, 2, 3, \dots$ ), it corresponds to SD, in which after each time interval  $\Delta t$  the chemical compositions are diluted by  $m = e^{\Delta t \bar{\phi}}$  fold, and  $s^{tot}(1 - \frac{1}{m})$  substrate is added at the beginning of the next cycle (where  $\bar{\phi}$  and  $\bar{\sigma}$  are the average dilution and influx rates over one division cycle; see Methods and Models for details). Similarly, a CSTR corresponds to an extreme case of a GD process where influx and dilution rates are constants:  $\phi(t) = \bar{\phi}$  and  $\sigma(t) = \bar{\sigma}$ . This also corresponds to an SD protocol with an infinitesimal short interval of cycles,  $\Delta t \rightarrow 0$  (see Methods and Models for details).

As the general case of GD protocols lies between the SD and CSTR protocols (see Fig. 2B), and CSTR is a special case of the SD, in the following sections, we will investigate the reaction dynamics of competing autocatalytic reaction sets (ACSs) under the SD protocol. Later we will return to the GD protocols and show that the condition for the bistability of the ACSs is bounded by the conditions obtained for the SD and the CSTR protocols.

## B. Nonlinearities are essential for two competing autocatalytic entities to exhibit heredity under serial dilution

First, we test whether an autocatalytic chemical reaction system can exhibit bistability under the SD protocol. We consider a simple class of autocatalytic reaction systems consisting of two identical (but distinguishable) autocatalytic entities,  $X_1$  and  $X_2$ , which consume the same substrate S (see Fig. 3A). This system can exhibit two distinct growth states. The rate equations for this class of systems are:

$$\frac{dx_i}{dt} = sr(x_i)x_i, \quad (1)$$

where  $i = 1, 2$ , and  $s$  is the concentration of the substrate S.  $r(x_i)$  is the reproduction rate of  $X_i$  as a function of  $x_i$  [49]. We assume  $r(x)$  is a differentiable and non-negative function for  $x \geq 0$ , but otherwise place no restrictions on its form. Later we will discuss realistic possibilities for  $r(x)$ .

We consider this reaction system under the SD protocol with cycle interval  $\Delta t$  and the dilution factor  $m (= e^{\bar{\phi}\Delta t})$  (see Methods and Models). The assumptions on the protocol from the previous section imply that the total concentration of the components  $s^{tot} = s + x_1 + x_2$  remains constant at  $s^{tot} = \frac{\bar{\sigma}}{\bar{\phi}}$ .

In the long timescale, after sufficiently many SD cycles, the trajectory of the chemical composition reaches a stationary periodic orbit (Fig. 3B). If the system does *not* exhibit inheritance, then it must settle into the same stable trajectory for every initial condition. As we assumed two ACSs which are completely symmetric, this trajectory must be one where the concentrations are equal (i.e.,  $x_1 = x_2$ ). In contrast, if there is the inheritance of the compositional state, then across different initial conditions, the system must exhibit bistability, i.e., two stable trajectories. Again, due to symmetry, in each of these two trajectories, one of the components,  $X_1$  or  $X_2$ , must be dominant. Therefore, a sufficient condition for bistability under the SD protocol can be obtained by showing the *instability* of the symmetrical ( $x_1 = x_2$ ) trajectory.

Introducing the notation  $\chi = x_1 + x_2$  and  $\delta = x_1 - x_2$ , for trajectories close to the symmetrical one we can assume that  $\delta \ll \chi$ . We can then derive the following relation (see details of the derivation in Appendix Sec. A 1):

$$\frac{\delta(t)}{\chi(t)} = \frac{r(\frac{\chi(t)}{2})}{r(\frac{\chi(0)}{2})} \frac{\delta(0)}{\chi(0)}. \quad (2)$$

If  $\delta(t)/\chi(t)$  at the end of a cycle,  $\delta(\Delta t)/\chi(\Delta t)$ , is larger than that at the beginning,  $\delta(0)/\chi(0)$ , the trajectory is unstable, otherwise it is stable. Therefore, the sufficient condition for bistability under the SD protocol is

$$r\left(\frac{\chi(\Delta t)}{2}\right) > r\left(\frac{\chi(0)}{2}\right). \quad (3)$$

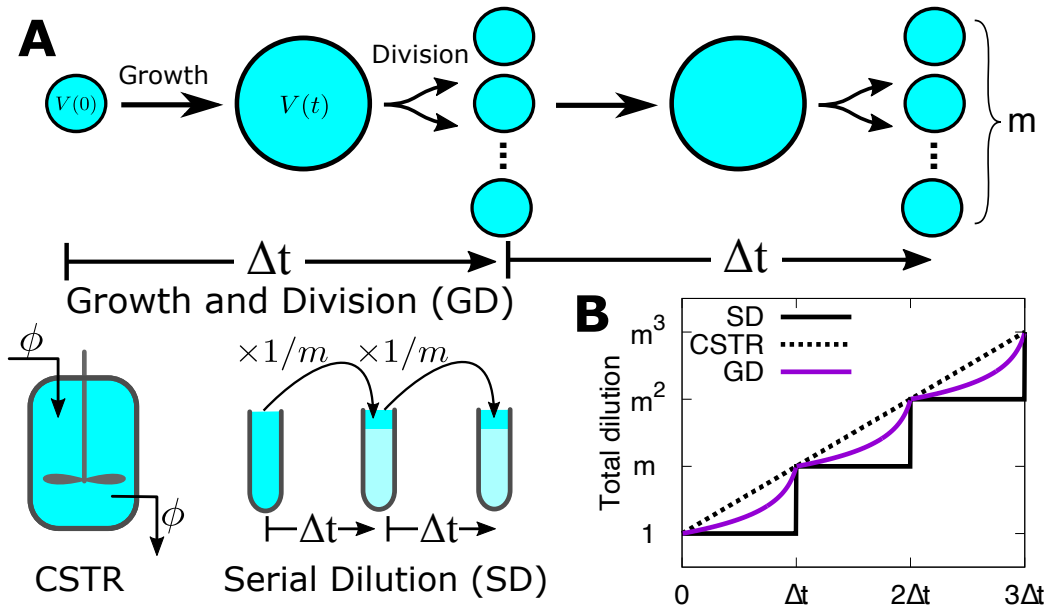


FIG. 2. (A) Schematic diagram of dilution protocols. Growth and Division (GD) cycles of a compartment with volume  $V(t)$ : After a period  $\Delta t$  during which the compartment grows, it divides into  $m$  smaller compartments each with volume  $m = e^{\bar{\phi}\Delta t}$  fold of the initial volume. Continuous Stirred-Tank Reactor (CSTR) protocol: a substrate is supplied, and compositions are diluted with the same constant rate  $\bar{\phi}$ . Serial Dilution (SD) protocol: each interval  $\Delta t$ , compositions are diluted with the factor  $m$ . (B) The time course of the total dilution inside the compartment undergoes (i.e.,  $\exp(\int_0^t \phi(t')dt')$ ). The black solid and dotted lines correspond to the serial dilution (SD) and continuous stirred-tank reactor (CSTR) protocols, respectively. The blue line corresponds to a case where the compartment grows at rate  $\frac{dV}{dt} \propto V^\alpha$  ( $\alpha = 4$ ) and splits into  $m$  equal-sized daughters when it divides (see Material and Methods).

That is, the stability of the compositional trajectory is determined by whether the reproduction rate at the end of a cycle  $r(\frac{x(\Delta t)}{2})$  is larger than that at the beginning  $r(\frac{x(0)}{2})$  or not [50].

For example, if  $r(x)x$  is linear, (e.g.,  $r(x)x = \epsilon + \kappa x$ , as is the case for the competitive *Azoarcus* ribozymes discussed later in Sec. II F 1) only the growth state with  $\delta = 0$  (i.e., the symmetrical trajectory) is always stable. Thus, for the system to show bistability and heredity,  $r(x)x$  must be a nonlinear function of  $x$ .

### C. Heredity of compositional state requires serial dilution interval to be below a critical threshold

Next, we analyze how bistability varies across the parameter space for the serial dilution (SD) protocol, consisting of the cycle interval  $\Delta t$  and the dilution factor  $m (= e^{\bar{\phi}\Delta t})$ . Here, we assume nonlinear reproduction rate functions that can show the bistability (i.e., satisfying the condition Eq. 3 under the appropriate SD protocol). In this subsection, we use  $r(x)x = \epsilon + \kappa x^2$  as an example of such a function. This function would be realized in a catalytic system consisting of two chemical reactions that generate each autocatalytic entity: a “spontaneous” or “background” chemical reaction where substrate S is converted to species X at a rate  $\epsilon$ , and a catalyzed re-

action where S is converted to X in the presence of another molecule of X with the efficiency  $\kappa$  (The square dependence of  $x$  is realized by dimeric catalyst [38], or multi-step reactions such as those in the modified *Azoarcus* system described later in Sec. II F 2.). However, the results in this subsection are true for all nonlinear functions of  $r(x)$  which are convex, i.e.,  $\frac{d^2 r}{dx^2} > 0$ .

Fig. 4A shows the bifurcation diagram of the concentrations just before a dilution in the stationary trajectory, as we vary the cycle interval  $\Delta t$  in the SD protocol while keeping the dilution rate  $\bar{\phi}$  fixed (note that the dilution factor  $m (= e^{\bar{\phi}\Delta t})$  is *not* fixed). The bifurcation occurs at  $\Delta t = \Delta t_c^{sd}$ . If  $\Delta t$  is more than this critical value, the system is no longer bistable, i.e., it does not exhibit heredity of the compositional state. Similarly, if we fix the interval  $\Delta t$  and vary the dilution rate  $\bar{\phi}$ , the same bifurcation at which the bistability disappears is observed at  $\bar{\phi} = \bar{\phi}_c^{sd}$  (Fig. 4C). The phase diagram of the parameters in the protocols,  $\Delta t$ , and  $\bar{\phi}$  is drawn in Fig. 4D.

The critical value  $\Delta t_c^{sd}$  depends on the reproduction rate function  $r(x)$  and its kinetic parameters (Fig. 4B). Using Eq. 3, the critical  $\Delta t$  at which the system loses bistability,  $\Delta t_c^{sd}$ , in a case with  $r(x)x = \epsilon + \kappa x^2$  is derived as  $\Delta t_c^{sd} \sim \frac{1}{\bar{\phi}} \log\left(\frac{\kappa}{4\epsilon}(s^{tot})^2\right)$  (Fig. 4B). Intuitively, we can realize this form as the condition that the background reaction dominates the catalyzed reaction at the start of each cycle (just after each dilution), i.e.,  $\epsilon > \kappa(x^*)^2$ , and

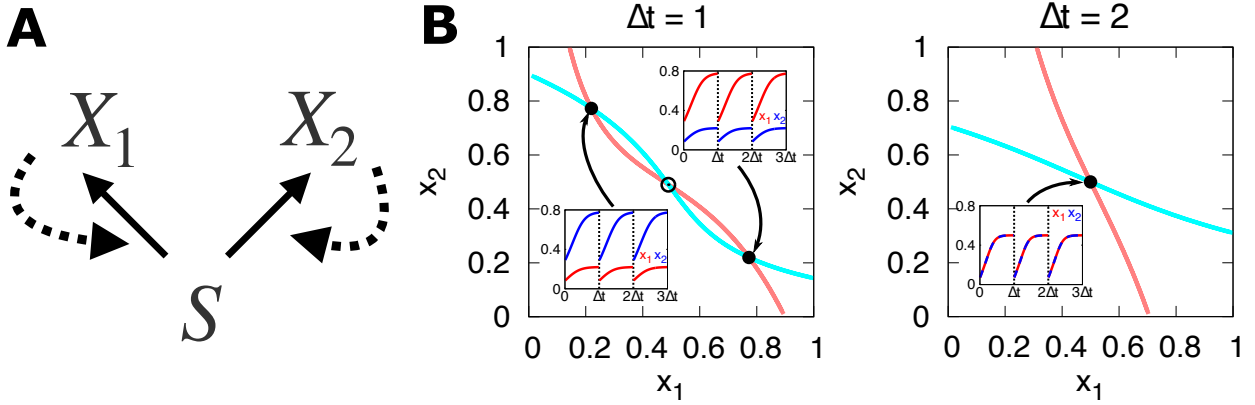


FIG. 3. (A) Schematics of the competing autocatalytic entities,  $X_1$  and  $X_2$ ; they are converted from a substrate  $S$  (solid arrows) catalyzed by itself (dashed arrows). (B) The red and blue curves represent the nullclines for the composition of the entities  $X_1$  and  $X_2$  at just before the dilution,  $x_1(-0)$  and  $x_2(-0)$ , respectively, in a case with  $r(x)x = \epsilon + \kappa x^2$ . The cross points represent the stable/unstable fixed points of concentrations of  $X_1$  and  $X_2$  at just before the dilution,  $x_1^*(-0)$  and  $x_2^*(-0)$ . See Methods and Models for the detail of the drawing of the nullclines. We set  $\Delta t = 1, 2$ ,  $\kappa = 8$ ,  $\epsilon = 0.5$ , and  $\bar{\phi} = 1$ .

$x^*$  is roughly  $x^* \sim \frac{1}{2} \frac{s^{tot}}{m}$  if all of the substrate  $S$  added at the beginning of a cycle is converted to the  $X_1$  or  $X_2$  by the end of the cycle.

The critical value for  $\bar{\phi}^{sd}$  is determined in a similar way. Especially, in the CSTR limit (i.e.,  $\Delta t \rightarrow 0$ ), the condition Eq. 3 becomes  $\frac{dr}{dx}(\frac{x^*}{2}) < 0$ , where  $\chi^*$  is such that  $\chi^* r(\frac{\chi^*}{2}) - \bar{\phi} = 0$  (see Appendix Sec A 2). Then, the critical dilution rate under CSTR,  $\phi_c^{cstr}$  is determined as  $\bar{\phi}$  such that breaks the above condition. In a case with  $r(x)x = \epsilon + \kappa x^2$ ,  $\phi_c^{cstr}$  is derived as  $\phi_c^{cstr} = 2s^{tot} \sqrt{\epsilon\kappa} - 4\epsilon$ .

#### D. Critical interval in a general growth and division process is bounded by that in the serial dilution protocol

Now, we return to the general GD protocols with the dilution rate  $\phi(t) = \frac{dV}{dt}/V$  discussed in Sec. A. Under such GD protocols, parametrized by cycle interval  $\Delta t$  and long-term dilution rate  $\bar{\phi}$ , similar to the SD protocol, we discuss the condition for the same ACSs to exhibit bistability.

Our main result is that the parameter region exhibiting bistability for the general GD protocol is bounded by that of SD and CSTR: if  $r(x)$  is a convex function of  $x$ , i.e.,  $\frac{d^2r}{dx^2} > 0$ , all of the parameter regions ( $\Delta t$  and  $\bar{\phi}$ ) where there is bistability under SD are included within the bistable region under the general dilution protocols, which in turn is included within the region exhibiting bistability under the CSTR protocol (see Appendix Sec. A 3 for the proof).

For example, we can consider the compartment growth dynamics obeying,  $\frac{dV}{dt} = \bar{\phi}_\alpha V^\alpha$ , where  $\alpha$  is the order of the growth, and  $\bar{\phi}_\alpha$  is a constant depending on  $\alpha$ . Here, to compare sensibly across the different protocols, we assume the growth rate of the compartment volume on

long timescales in each case is the same, i.e., SD with the dilution factor  $m = e^{\bar{\phi}\Delta t}$  or the CSTR with the dilution rate  $\bar{\phi}$  (see Methods and Models for the details). As Fig. 5 shows, the critical interval  $\Delta t_c$  that is the upper limit for a system with bistability in the general case is bounded from below by the critical  $\Delta t_c^{sd}$  for the SD protocol:  $\Delta t_c^{sd} \leq \Delta t_c < \Delta t_c^{cstr}$ , under the fixed  $\bar{\phi}$ , where  $\Delta t_c^{cstr}$  is infinite or otherwise zero ( $\Delta t_c^{cstr} = 0$  means that there is no bistability under any  $\Delta t$  values). On the other hand, if  $\Delta t$  is fixed,  $\phi_c^{sd} \leq \phi_c \leq \phi_c^{cstr}$ , where  $\phi_c^{sd}$ ,  $\phi_c^{cstr}$  and  $\phi_c$  are the threshold for  $\phi$  under SD, CSTR and general protocols, respectively.

#### E. Robustness of results

Two key results we have are: (i) for a serial dilution protocol, there is a critical dilution interval and dilution rate for the inheritance to be possible, (ii) these critical values provide bounds for the properties of a general growth and division process in order to enable inheritance. We have checked the robustness of these results to a number of variations and extensions of our models, namely:

1. Autocatalytic sets with reversible chemical reactions (Appendix Sec. B 1)  
Making all reactions reversible is more chemically realistic and allows convergence to thermal equilibrium in the absence of dilution protocols. Interestingly, we find that, unlike the irreversible reaction case, the region of bistability is bounded in the reversible case for the parameter  $\bar{\phi}$ . That is, for the SD protocol with fixed  $\Delta t$ , there is both an upper and a lower critical  $\bar{\phi}$  (see Fig. S3 in Appendix). Importantly, even with reversible reactions, the parameter space for the general GD

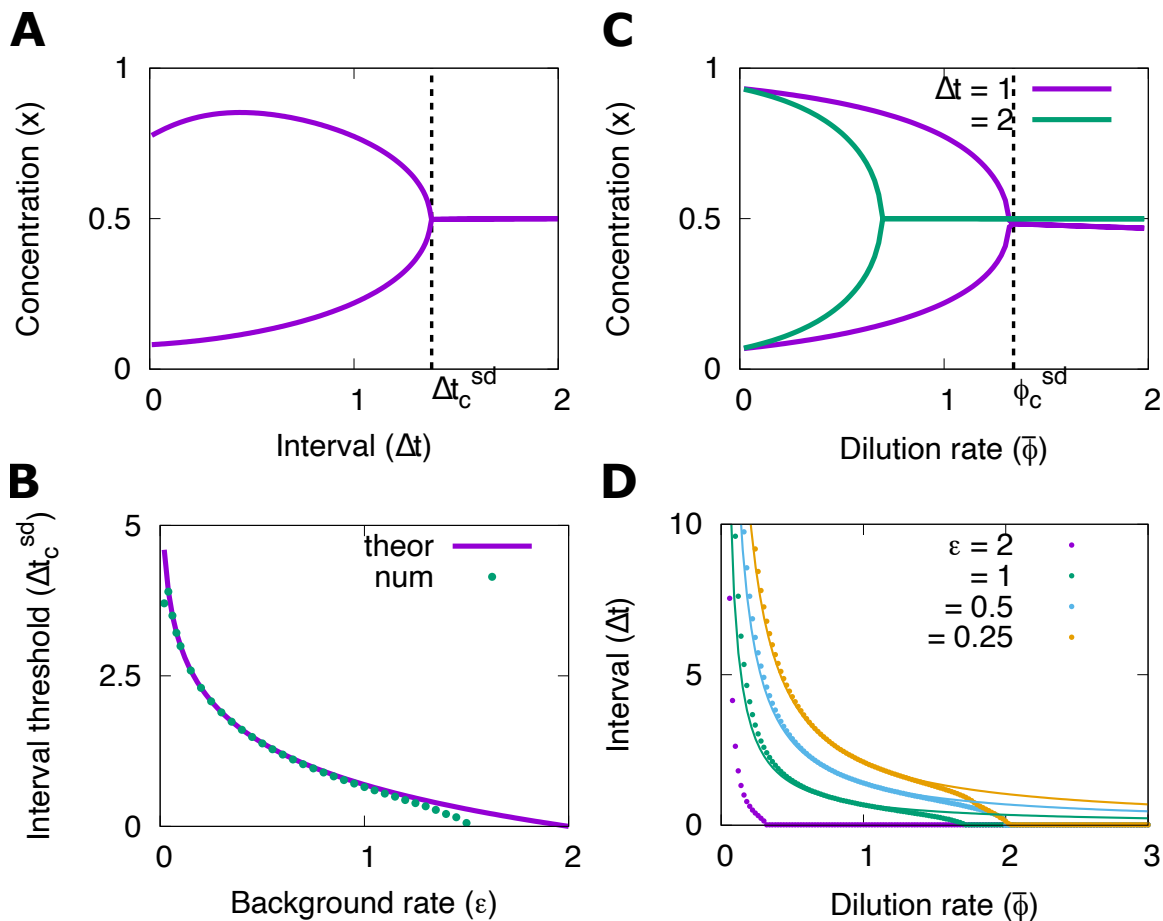


FIG. 4. (A) The bifurcation diagram with a varying interval of each dilution cycle  $\Delta t$  in a case with  $r(x)x = \epsilon + \kappa x^2$ . The pitchfork bifurcation occurs at  $\Delta t = \Delta t_c^{sd}$  when the upper and lower fixed points merge into one fixed point. (B) The dotted line represents the critical point  $\Delta t_c^{sd}$ , which divides the regions where the system has bistability or not. The solid line represents the theoretical line for  $\Delta t_c^{sd}$  determined by the relation:  $\Delta t_c^{sd} \sim \frac{1}{\bar{\phi}} \log\left(\frac{\kappa}{4\epsilon}(s^{tot})^2\right)$ . (C) The bifurcation diagram with a varying long-term dilution rate  $\bar{\phi}$ . (D) The dotted line represents the critical point  $\Delta t_c^{sd}$ , which divides the regions where the system has bistability or not. Each colored dotted line represents the difference in the background reaction rate  $\epsilon$ . The theoretical lines (solid) are the same as in (B). We set the default parameters as  $\epsilon = 0.5$ ,  $\kappa = 8$  and  $\bar{\phi} = 1$ .

protocol contains that for SD protocols, as we found for irreversible reactions.

## 2. ACSs with asymmetric kinetic rates (Appendix Sec. B 2)

Our results are similar even when the two competing ACSs have different kinetic rate constants (catalytic efficiency), although the bifurcation where the bistability disappears is discontinuous (see Fig. S4). The boundary in the parameter space for ACSs that have bistability under general GD protocols is also bounded by the boundaries for the SD and CSTR protocols (see Appendix).

## 3. Reproduction rates that depend on both entities (Appendix Sec. B 3)

The rate equation Eq. 1 and the condition Eq. 3 can be

extended to a more general reproduction rate function  $r(x_1, x_2)$ , which also depends on the concentration of the other entity; for example, this includes mutual inhibition between the entities. Our results are unchanged by this generalization.

## 4. Stochasticity in reaction systems or protocols (Appendix Sec. B 4)

If the number of molecules is small (e.g., the reaction dynamics occur inside sufficiently small compartments), stochastic fluctuations are not negligible. Close to the deterministic bifurcation transitions, these fluctuations cause random transitions between states, which destroys the information to be inherited. Thus, the parameter space where the system has heredity is narrower than the deterministic case. However, the existence of a critical threshold in the dilution interval or the dilution rate

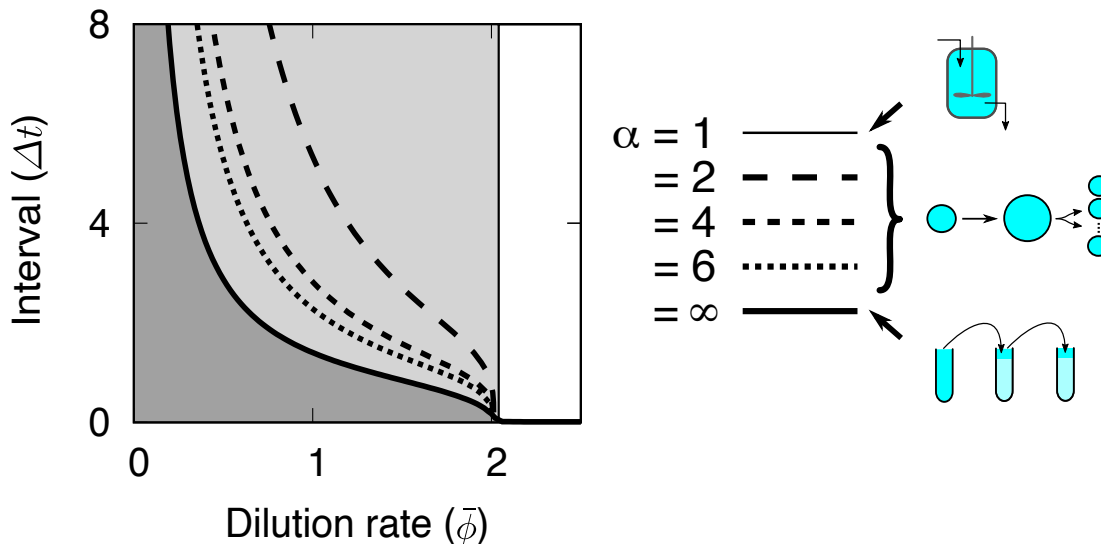


FIG. 5. Phase diagram for the system with/without heredity using the dilution rate  $\bar{\phi}$  and dilution interval  $\Delta t$  as parameters, in a case with  $r(x)x = \epsilon + \kappa x^2$ . The solid line represents the boundary between with and without bistability under SD. The dashed lines represent that under the GD with different growth laws (the exponents  $\alpha$  of the growth law for compartment;  $\alpha = 2, 4, 6$ ). The vertical thin line represents that under GD with  $\alpha = 1$ , corresponding to the CSTR protocol. We set the parameters as  $\kappa = 8, \epsilon = 0.5$ .

and the bistable parameter region for general GD cycles being bounded by that of SD and CSTR, are robust to the addition of stochastic noise in the chemical reaction system. The results are also robust to stochasticity in the dilution protocols; for example, if the division time  $\Delta t$  is randomly distributed (see Appendix Sec. B 4 b).

5. Differential reproduction of different chemical compositional states (Appendix Sec. B 5)

Finally, we investigated situations where the dilution rates depend on the chemical composition, and the system has different growth rates for the two growth states. As noted in the introduction, this is, in fact, a crucial property necessary for a population of compartmentalized chemical reaction systems to undergo Darwinian evolution. We consider cases where  $\phi$  depends both symmetrically or asymmetrically on  $x_1$  and  $x_2$ . We have also checked the case where the division interval, not the rate, depends on the chemical composition. In all cases, our results continue to hold.

### F. Autocatalytic sets based on the *Azoarcus* ribozyme

In this section, we apply the framework we have developed to an experimentally realized ACS based on the *Azoarcus* ribozyme [30, 47, 48]. We examine a few simplifications and variants of this ribozyme system, along with systems consisting of two *Azoarcus* ribozymes competing for the same nutrients. We show that some of these variants can exhibit two (exponential) growth states, and some are not. In particular, we find a modified version

of the *Azoarcus* ribozyme, which incorporates additional catabolic steps [51], can exhibit bistability under competition for shared resources. Applying our results on critical thresholds to this system, we can suggest a serial dilution protocol that can test whether this modified *Azoarcus* system can exhibit the inheritance of its phenotypic state.

The *Azoarcus* ribozyme **WXYZ** can be assembled from two fragments by the reaction,



${}_M\mathbf{WXY}_N$  and  $\mathbf{Z}$  are the fragments, and M and N are bases at the ends of **WXY** [52]. M and N can be arbitrary bases {A, U, C, G}, thus there are 16 different types of this engineered *Azoarcus* ribozyme. This reaction is catalyzed specifically by a ribozyme if M in the fragment is a complementary base to N in the ribozyme. Certain types of the ribozyme can catalyze the formation reaction of themselves: e.g.,  ${}_M\mathbf{WXY}_N\mathbf{Z}$  such that  $M = C$  and  $N = G$  or  $M = U$  and  $N = A$ . Besides being catalyzed by the corresponding ribozymes, the reaction is also (weakly) catalyzed by a non-covalent complex between the corresponding fragments, or non-specifically by non-corresponding ribozymes; we call these ‘background reactions’ [48].

#### 1. Absence of bistability in competing ACSs based on the original engineered *Azoarcus* ribozyme

We imagine a particular case of the system in Fig. 6A, where  $X_1$  and  $X_2$  are two distinct types of self-catalyzing

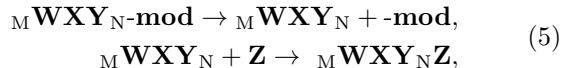
*Azoarcus* ribozyme, made from two distinct **WXY** fragments and a common **Z** fragment. For simplicity, we assume the two sets of reactions occur with symmetric kinetic rates. We assume the **WXY** fragments are abundant, whereas **Z** is not and limits the reaction rates. Thus, **Z** acts as the common substrate S.

Then, the rate equations for the concentrations of  $X_1$  and  $X_2$ ,  $x_1$  and  $x_2$  are described as Eq. 1 with the linear reproduction function  $r(x)x = \epsilon + \kappa x$ , where  $\epsilon$  is the rate constant of the background reaction, and  $\kappa$  is the catalytic strength of  $X_1$  and  $X_2$ . [53] As mentioned earlier, for simplicity, we assume the catalytic efficiency of  $X_1$  and  $X_2$  are equal.

As already discussed in Sec. B, competing ACSs with such linear reproduction rate functions cannot be bistable – for all initial conditions, the system eventually reaches the state with an equal amount of the two ribozymes. More precisely, in Sec. B, only the local stability of the symmetric state is shown. In this case, however, we can further show the *global* stability of this symmetric state [54]. Therefore, the system has no heredity, which is consistent with previous experiments [30].

### 2. *Azoarcus* system coupled with metabolism exhibits bistability

As discussed in Sec. B, a reproduction rate function  $r(x)$  with a higher order of catalysis is necessary for bistability. In the *Azoarcus* system, this has previously been realized by engineering a variant where the system is coupled to catabolism and anabolism reactions:



where **-mod** represents an extra sequence joined to fragments **WXY**. Here, the first reaction represents a catabolism reaction that processes the modified fragment to a substrate that can participate in ribozyme synthesis. The second one represents an anabolic reaction that joins the fragments to form the ribozyme. We denote **Z** as S, **WXYZ** as  $X_1$  and  $X_2$  and **WXY** as  $X'_1$  and  $X'_2$ . Two ribozymes  $X_1$  and  $X_2$  synthesize themselves from the shared substrate S, and there is the intermediate state  $X'_1$  and  $X'_2$  during the synthesis (see Fig. 6B).

The concentrations of chemical species obey the rate equations

$$\begin{aligned} \frac{dx'_i}{dt} &= (\epsilon + \kappa x_i)(1 - (1 + b)sx'_i + bx_i), \\ \frac{dx_i}{dt} &= (\epsilon + \kappa x_i)(sx'_i - bx_i), \end{aligned} \quad (6)$$

where  $i = 1$  or  $2$ ,  $\epsilon$  is the spontaneous reaction rate,  $\kappa$  is the catalytic efficiency of the ribozymes, and  $b$  ( $\ll 1$ ) is the relative rate of backward reaction compared with the forward one [55]. We again consider the ACSs system

under the SD protocol with the interval  $\Delta t$  and an  $m$ -fold dilution factor. Also, the total concentration of S,  $X_1$  and  $X_2$  is kept as a constant  $s^{tot} = s + x_1 + x_2$ .

In contrast with the original system (Fig. 6A), this system indeed exhibits bistability for appropriate values of the parameters  $\Delta t$  and  $\bar{\phi}$  (Fig. S12), i.e., it reaches either the  $X_1$ -dominated state or the  $X_2$ -dominated state, depending on the initial composition of the species (Fig. 6C).

### 3. Bounds on the critical $\Delta t$ and $\bar{\phi}$ for observing inheritance of compositional state

As in the previous models, there is the region for the kinetic parameters,  $\Delta t$  and  $\bar{\phi}$ , where the system exhibits bistability (see Fig. 6D). For this modified *Azoarcus* system, the concrete value that would exhibit heredity under SD is predicted that the dilution interval lies within 50-125 min, and the dilution factor per cycle lies between 2.5-11-fold (We assumed  $\kappa = 0.1\mu\text{M}^{-2}\text{min}^{-1}$ ,  $\epsilon = 0.01\mu\text{M}^{-1}\text{min}^{-1}$ ,  $\bar{\phi} = 0.04\text{min}^{-1}$  and  $b = 0.1$ ; see Fig. S13)

Further, we checked numerically (see Fig. 6D and Appendix Sec. C) that under the alternative dilution protocols (various functions of  $\phi(t)$ ) upper bound of  $\Delta t$  for the bistability is bounded by  $\Delta t_c^{sd}$ . These results for the *Azoarcus* based system are robust even if the reaction network is modified: we have tested alternative structures, asymmetric kinetic rates, and stochastic reactions or compartment dynamics (see Appendix Sec. D).

## III. DISCUSSION

We have studied mathematical models of a very general class of chemical reaction systems consisting of two ACSs competing for a shared resource. When enclosed within growing and dividing compartments, such a system is one of the simplest capable of exhibiting the heredity of its compositional state. In other words, it can exhibit two distinct compositional states that are stable to the growth and division of the compartment. This, along with differential reproduction rates and some sources of variation of the compositional state, is a key property for a chemical system to form a Darwinian population.

Our main result is that such bistable chemical systems exhibit the heredity of their two compositional states when the growth and division cycle parameters lie within certain critical bounds. These are bounded by the critical values for these parameters in a serial dilution protocol. Thus, a serial dilution experiment, which is much easier to set up in a laboratory than a general growth and division scenario, can be used to test whether a given autocatalytic chemical system can exhibit heredity of its compositional states.

We used these results to analyze a chemical system based on the *Azoarcus* ribozyme, which has been real-



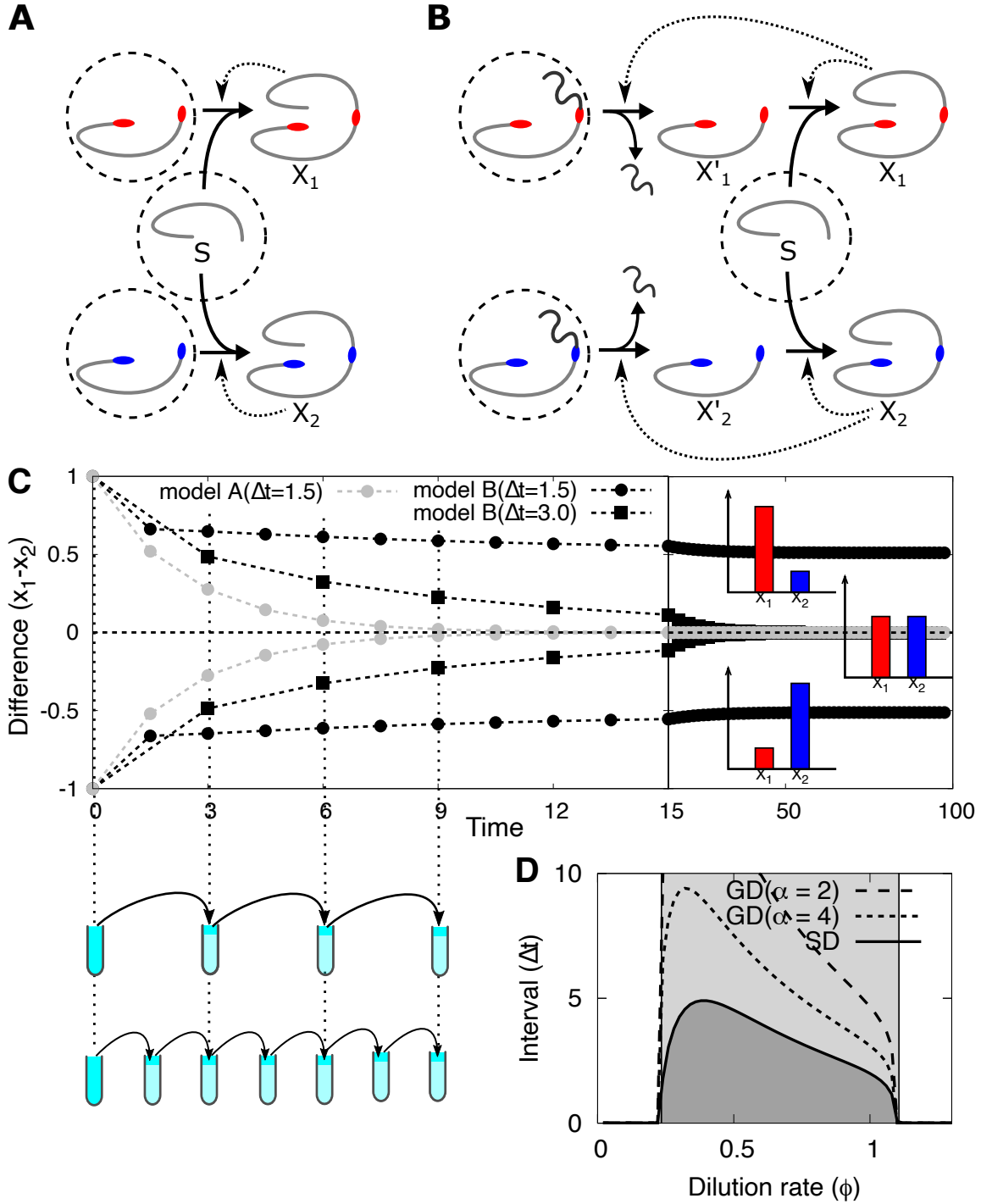


FIG. 6. Schematic diagram of the model chemical reaction systems: (A) non-modified two competing autocatalytic ribozymes and (B) the ones coupled with anabolism and catabolism reactions. Solid arrows represent reactions and dashed represent catalysis. Species enclosed by dashed circles are supplied from outside. (C) Time course of the difference of the concentration of the ribozyme species,  $\delta = x_1 - x_2$ , starting from the initial condition where  $\delta = 1$  or  $= -1$ . The gray circle represents the time course for the model (A) under the SD protocol with the interval  $\Delta t = 1.5$  (Eq. 4 with  $r(x)x = \epsilon + \kappa x$ ; we considered the reversible reaction). The black circle and square represent time courses for the model (B) under the SD with  $\Delta t = 1.5$  and  $= 3.0$ , respectively. We set  $\epsilon = 0.25$ ,  $\kappa = 2.5$ , and  $b = 0.1$ . (D) The parameter region for the system with the bistability. In the dark-grey area, the system has bistability under SD protocol. The thin vertical lines (the boundaries for the light-grey area) represent the lower and upper boundary for  $\bar{\phi}$  for the bistability under the CSTR. We set  $\epsilon = 0.25$ ,  $\kappa = 2.5$ , and  $b = 0.1$ .

ized experimentally, and predicted that it would indeed exhibit heredity under serial dilution for a specific range of values for the dilution interval and dilution factor (see Results section II F 3). The *Azoarcus* system is a particularly intriguing experimental system for studying heredity because it can go beyond our present theoretical analysis in two ways:

(i) It can be engineered to exhibit any number of compositional states. For example, by choosing bases M and N to be AU, UA, CG, and GC, one can have four ACSs competing for the same resource. Such a system can encode more than 1-bit of information [56].

(ii) Each compositional state can be composed of a large number of chemical species. The *Azoarcus* ribozyme can catalyze not only the formation of itself but also the production of diverse RNA sequences [57]. Here, self-reproducing ribozymes (ACSs) correspond to the ‘autocatalytic cores,’ and the sequences produced by the ribozyme correspond to their ‘peripheries’ [25, 58, 59]. Species in the periphery can nevertheless play important roles, for instance, in the differential reproduction of the compositional states.

Of course, extending our present theoretical analysis to multistable systems which can encode more than 1-bit of information and to more complex autocatalytic systems consisting of cores and peripheries is relatively straightforward, and easy to be implemented experimentally. The *Azoarcus* system can guide such theoretical extensions, but we expect our core results to remain the same for such more complex reaction systems.

The condition for bi/multistability of autocatalytic systems has been previously discussed in the context of self-reproduction and the origins of life. For example, Giri-Jain [40] found a class of ACSs that exhibit bistability under CSTR conditions, with one state growing and the other a non-growing state [41]. Remarkably, their network model also needs two steps to show bistability (if mass-action kinetics is assumed), like the *Azoarcus* system coupled to metabolic reactions. Note that the bistability in their model needs high catalytic efficiency of self-catalysts (e.g.,  $10^4$  order of magnitude) [60]. It is noteworthy that our model exhibits bistability even with relatively low efficiency of catalysts (or equivalently, with a high rate of background reactions), which is more plausible for a prebiotic scenario.

Some previous studies have shown how heredity of composition can arise even without bistability due to the difference in reproduction rate and competition between compartments. For example, see Segre-Lancet [23], Kaneko-Yomo [61], or Doulier et al. [62], for the models with ‘multilevel selection’ [63] (including ‘transient compartmentalization’ [64]). However, such mechanisms require fine-tuning for protocols, such as the size of compartments, and it is controversial whether the compositional states can be sustained enough for selection pressures to act on them [24]. In contrast, we demonstrated that compositional information in our models is robustly inherited in a single lineage of compartments across a

wide range of values for kinetic constants or protocol parameters. Note that compartments such as coacervates are known for their high permeability, and they exchange their contents (including large ribozymes) at faster rates. Even in such a case, the inheritance of compositional information could be robust for the kind of bistable systems we have studied. [65].

## IV. METHODS AND MODELS

### A. Simulation details

All simulations of chemical reaction dynamics involved solving ordinary differential equations (and a discrete mapping). This was done using the adaptive Runge-Kutta method (Dormand-Prince method) coded by the C++ language [66].

*The serial dilution protocol:* The composition of entities  $x_1(t), x_2(t), \dots, x_M(t)$  under the serial dilution (SD) protocol evolve according to a rate equation,

$$\frac{d\mathbf{x}}{dt} = \mathbf{f}(\mathbf{x}), \quad (7)$$

where  $\mathbf{x}(t)$  is a time-dependent compositional vector (e.g., in a case with a model in Sec. II F,  $\mathbf{x}(t) = \{s(t), x'_1(t), x'_2(t), x_1(t), x_2(t)\}$ ). At each interval  $t = n\Delta t$  ( $n = 1, 2, \dots$ ), the all entities are diluted (and the substrate S is added), that is, the composition change by a discrete mapping:

$$\mathbf{x}(n\Delta t + 0) = \frac{1}{m}\mathbf{x}(n\Delta t - 0) + s^{tot}(1 - \frac{1}{m})\hat{\mathbf{1}}_s, \quad (8)$$

where  $\hat{\mathbf{1}}_s$  is a unit vector for the substrate S (e.g., in a case with a model in Sec. II F,  $\hat{\mathbf{1}}_s = \{1, 0, 0, 0, 0\}$ ),  $n = 0, 1, \dots$ , and  $n\Delta t - 0$  and  $n\Delta t + 0$  represent the time right before and after the dilution at  $t = n\Delta t$  ( $n = 0, 1, \dots$ ). If the reaction dynamics in Eq. 14 does not change the total sum of composition,  $x^{tot} = \sum_i x_i$ , the repeats of the dilution cycle, i.e., the mapping in Eq. 15 results in the steady state with  $x^{tot} = s^{tot}$ . In the main text, we fix  $x^{tot}$  as  $s^{tot}$ , and the concentration of free substrate is  $s = s^{tot} - \sum x_i$  in the rate equations.

If we set  $\Delta t$  enough small, i.e., the system is diluted repeatedly at quite a short interval, and set  $m$  and  $s^{tot}$  as  $m = e^{\phi\Delta t}$  and  $s^{tot} = \frac{\bar{\sigma}}{\phi}$ , the dynamics and the steady-state of the species are the same as that in the continuous stirred-tank reactor (CSTR) with a dilution rate  $\phi$  and a substrate supply rate  $\bar{\sigma}$  [45].

*The dilution by the growth of the compartment:* Formally, the rate equation for the chemical composition  $\mathbf{x}$  under the general dilution protocols is expressed as,

$$\frac{d\mathbf{x}}{dt} = \sigma(t)\hat{\mathbf{1}}_s + \mathbf{f}(\mathbf{x}) - \phi(t)\mathbf{x}, \quad (9)$$

where  $\mathbf{f}(\mathbf{x})$  is an arbitrary reaction dynamics, and  $\sigma(t)$  and  $\phi(t)$  is the time-dependent supply rate of S and the

dilution rate. If  $\sigma(t) = \phi(t)$  and the dynamics  $\mathbf{f}(\mathbf{x})$  conserves the total concentration  $x^{tot}$ , then  $x^{tot}$  is constant at the steady state.

In the case of the compartment growth scenario,  $\phi(t)$  is determined as  $\phi(t) = \frac{dV}{dt}/V$ , where  $V$  is the volume of the compartment. For example, we can consider the arbitrary order of compartment growth.

$$\frac{dV}{dt} = \bar{\phi}_\alpha V^\alpha, \quad (10)$$

where  $\alpha$  is the order of the growth, and  $\bar{\phi}_\alpha$  is a constant depending on  $\alpha$ . If  $\alpha = 1$ , the growth is exponential. For example, if we consider the volume growth is proportional to the surface area, i.e.,  $\frac{dV}{dt} = r_\alpha S$ , and if the vesicle is spherical, the surface area  $S$  is  $S = V^{\frac{2}{3}}$ , then  $\alpha = 2/3$  [67, 68]. The volume  $V$  is solved as  $V(t) = (\bar{\phi}_\alpha(1-\alpha)t + V_0^{1-\alpha})^{\frac{1}{1-\alpha}}$ . Here, we assume the growth speed of compartment's volume in the long time scale is the same as the exponential growth with rate  $\bar{\phi}$  (i.e., CSTR with dilution rate  $\bar{\phi}$ ); that is,  $V(\Delta t) = V_0 e^{\bar{\phi}\Delta t}$ . Then,  $\bar{\phi}_\alpha$  should be  $\bar{\phi}_\alpha = \frac{V_0^{1-\alpha}}{(1-\alpha)\Delta t} (e^{\bar{\phi}(1-\alpha)\Delta t} - 1)$ . Therefore, the dilution rate is

$$\phi(t) = \frac{e^{\bar{\phi}(1-\alpha)\Delta t} - 1}{(1-\alpha)\Delta t (1 + \frac{t}{\Delta t} (e^{\bar{\phi}(1-\alpha)\Delta t} - 1))}. \quad (11)$$

Note that  $\phi(t)$  approaches  $\phi(t) = \bar{\phi}$  as  $\alpha \rightarrow 1$  (i.e., the same as the condition under the CSTR). On the other

hand,  $\phi(t)$  approaches  $\phi(t) = \infty$  if  $t = n\Delta t$  ( $n = 1, 2, \dots$ ) or  $\phi(t) = 0$  if otherwise as  $\alpha \rightarrow \infty$  (i.e., the serial dilution condition).

*Nullclines under SD protocol:* The map between the chemical composition at the beginning (end) of one cycle to that at the beginning (end) of the next cycle,  $P: \mathbf{x}(n\Delta t + 0) \mapsto \mathbf{x}((n+1)\Delta t + 0)$ ,  $n = 0, 1, \dots$ , is interpreted as the Poincaré map obtained using the Poincaré section:  $t = n\Delta t$ . The trajectory  $\mathbf{x}(t)$  is stable if and only if the corresponding fixed point in the Poincaré map is stable. Then, the stability of the trajectories can be determined from the intersections of the nullclines of the discrete map (see Fig. 3B for a depiction of these nullclines). The nullcline for  $X_1$ ,  $x_1 = f(x_2)$ , is obtained by the fixing the concentration of  $X_2$  at the beginning of every cycle,  $x_2(n\Delta t + 0) = x_2$ , and calculating the stationary concentration of  $X_1$  at the beginning of cycles  $x_1 = x_1^*(+0)$  by repeating the map enough times.

## ACKNOWLEDGMENTS

We thank Sanjay Jain and Angad Yuvraj for the fruitful discussions. We acknowledge support from the Indo-French Centre for the Promotion of Advanced Research under project no. 5904-3, the Department of Atomic Energy (India) under project no. RTI4006, the Simons Foundation (Grant No. 287975), and computational facilities at NCBS.

- 
- [1] C. R. Woese, The genetic code :the molecular basis for genetic expression., Proc. Natl. Acad. Sci. U.S.A (1967).
- [2] F. H. Crick, The origin of the genetic code, J. Mol. Biol. **38**, 367 (1968).
- [3] A. G. Cairns-Smith, The origin of life and the nature of the primitive gene, Journal of Theoretical Biology **10**, 53 (1966).
- [4] W. Gilbert, Origin of life: The rna world, nature **319**, 618 (1986).
- [5] S. A. Kauffman, Autocatalytic sets of proteins, Journal of Theoretical Biology **119**, 1 (1986).
- [6] S. Jain and S. Krishna, Autocatalytic sets and the growth of complexity in an evolutionary model, Physical Review Letters **81**, 5684 (1998).
- [7] A. Blokhuis, D. Lacoste, and P. Nghe, Universal motifs and the diversity of autocatalytic systems, Proceedings of the National Academy of Sciences **117**, 25230 (2020).
- [8] S. Ameta, Y. J. Matsubara, N. Chakraborty, S. Krishna, and S. Thutupalli, Self-reproduction and darwinian evolution in autocatalytic chemical reaction systems, Life **11**, 308 (2021).
- [9] P. Adamski, M. Eleveld, A. Sood, Á. Kun, A. Szilágyi, T. Czárán, E. Szathmáry, and S. Otto, From self-replication to replicator systems en route to de novo life, Nature Reviews Chemistry **4**, 386 (2020).
- [10] R. Mizuuchi and N. Ichihashi, Primitive compartmentalization for the sustainable replication of genetic molecules, Life **11**, 191 (2021).
- [11] I. A. Chen, R. W. Roberts, and J. W. Szostak, The emergence of competition between model protocells, Science **305**, 1474 (2004).
- [12] D. Zwicker, R. Seyboldt, C. A. Weber, A. A. Hyman, and F. Jülicher, Growth and division of active droplets provides a model for protocells, Nature Physics **13**, 408 (2017).
- [13] M. C. Boerlijst and P. Hogeweg, Spiral wave structure in pre-biotic evolution: hypercycles stable against parasites, Physica D: Nonlinear Phenomena **48**, 17 (1991).
- [14] P. Szabó, I. Scheuring, T. Czárán, and E. Szathmáry, In silico simulations reveal that replicators with limited dispersal evolve towards higher efficiency and fidelity, Nature **420**, 340 (2002).
- [15] M. S. Krieger, S. Sinai, and M. A. Nowak, Turbulent coherent structures and early life below the kolmogorov scale, Nature communications **11**, 1 (2020).
- [16] S. Charlat, A. Ariew, P. Bourrat, M. Ferreira Ruiz, T. Heams, P. Huneman, S. Krishna, M. Lachmann, N. Lartillot, L. Le Sergeant d'Hendecourt, *et al.*, Natural selection beyond life? a workshop report, Life **11**, 1051 (2021).
- [17] P. Godfrey-Smith, Conditions for evolution by natural selection, The Journal of Philosophy **104**, 489 (2007).
- [18] R. C. Lewontin, The units of selection, Annual Review

- of Ecology and Systematics , 1 (1970).
- [19] J. A. Endler, *Natural Selection in the Wild.(MPB-21), Volume 21* (Princeton University Press, 2020).
- [20] M. Ridley, *Evolution, 3rd Edition* (Wiley-Blackwell, 2003).
- [21] This could occur via a variety of mechanisms. For example, osmotic pressure due to the difference in the composition between the inside and outside of the compartment may induce its growth [11]. The ACS could also produce the precursors of the compartment (e.g., lipid molecules) [69, 70]. Another possibility is that the ACS energetically drives the growth, and shape instability triggers the division of compartments [12].
- [22] In dynamical systems, stability often refers to stability against random stochasticity, e.g., due to thermal noise. It is true that for an autocatalytic chemical system to exhibit an inheritance of its phenotype (its chemical composition), it must also exhibit a certain amount of stability against noise. Some small enough probability of transitions to different states due to noise can be subsumed under phenotypic variation (indeed, this may be the only source of variation available), but too much will destroy the property of the heredity of states. Later we provide some results from stochastic simulations, but we largely assume that if the system, in the absence of noise, is stable upon division, then it satisfies the third property of inheritance of phenotypic traits.
- [23] D. Segré, D. Ben-Eli, and D. Lancet, Compositional genomes: prebiotic information transfer in mutually catalytic noncovalent assemblies, *Proceedings of the National Academy of Sciences* **97**, 4112 (2000).
- [24] V. Vasas, E. Szathmáry, and M. Santos, Lack of evolvability in self-sustaining autocatalytic networks constrains metabolism-first scenarios for the origin of life, *Proceedings of the National Academy of Sciences* **107**, 1470 (2010).
- [25] V. Vasas, C. Fernando, M. Santos, S. Kauffman, and E. Szathmáry, Evolution before genes, *Biology direct* **7**, 1 (2012).
- [26] W. Hordijk, M. Steel, and S. Kauffman, The structure of autocatalytic sets: Evolvability, enablement, and emergence, *Acta Biotheoretica* **60**, 379 (2012).
- [27] N. Guttenberg, M. Laneville, M. Ilardo, and N. Aubert-Kato, Transferable measurements of heredity in models of the origins of life, *PLoS one* **10**, e0140663 (2015).
- [28] D. Lancet, R. Zidovetzki, and O. Markovitch, Systems protobiology: origin of life in lipid catalytic networks, *Journal of The Royal Society Interface* **15**, 20180159 (2018).
- [29] I. Colomer, A. Borissov, and S. P. Fletcher, Selection from a pool of self-assembling lipid replicators, *Nature Communications* **11**, 1 (2020).
- [30] S. Ameta, S. Arsène, S. Foulon, B. Saudemont, B. E. Clifton, A. D. Griffiths, and P. Nghe, Darwinian properties and their trade-offs in autocatalytic rna reaction networks, *Nature Communications* **12**, 1 (2021).
- [31] Z. Peng, J. Linderöth, and D. A. Baum, The hierarchical organization of autocatalytic reaction networks and its relevance to the origin of life, *PLOS Computational Biology* **18**, e1010498 (2022).
- [32] T. S. Gardner, C. R. Cantor, and J. J. Collins, Construction of a genetic toggle switch in *escherichia coli*, *Nature* **403**, 339 (2000).
- [33] J. E. Ferrell Jr and W. Xiong, Bistability in cell signaling: How to make continuous processes discontinuous, and reversible processes irreversible, *Chaos: An Interdisciplinary Journal of Nonlinear Science* **11**, 227 (2001).
- [34] Z. Peng, A. M. Plum, P. Gagrani, and D. A. Baum, An ecological framework for the analysis of prebiotic chemical reaction networks, *Journal of Theoretical Biology* **507**, 110451 (2020).
- [35] F. C. Frank, On spontaneous asymmetric synthesis, *Biochimica et biophysica acta* **11**, 459 (1953).
- [36] G. Laurent, D. Lacoste, and P. Gaspard, Emergence of homochirality in large molecular systems, *Proceedings of the National Academy of Sciences* **118**, e2012741118 (2021).
- [37] I. Maity, N. Wagner, R. Mukherjee, D. Dev, E. Peacock-Lopez, R. Cohen-Luria, and G. Ashkenasy, A chemically fueled non-enzymatic bistable network, *Nature Communications* **10**, 1 (2019).
- [38] N. Wagner, R. Mukherjee, I. Maity, S. Kraun, and G. Ashkenasy, Programming multistationarity in chemical replication networks, *ChemSystemsChem* **2**, e1900048 (2020).
- [39] F. Schlögl, Chemical reaction models for non-equilibrium phase transitions, *Zeitschrift für physik* **253**, 147 (1972).
- [40] V. Giri and S. Jain, The origin of large molecules in primordial autocatalytic reaction networks, *PLoS ONE* **7**, e29546 (2012).
- [41] Y. J. Matsubara and K. Kaneko, Optimal size for emergence of self-replicating polymer system, *Physical Review E* **93**, 032503 (2016).
- [42] T. Wilhelm, The smallest chemical reaction system with bistability, *BMC systems biology* **3**, 1 (2009).
- [43] G. Craciun, Y. Tang, and M. Feinberg, Understanding bistability in complex enzyme-driven reaction networks, *Proceedings of the National Academy of Sciences* **103**, 8697 (2006).
- [44] The necessary conditions for bistable chemical reactions are: (i) positive feedback (e.g., autocatalysis), (ii) filtering noise, and (iii) preventing explosion (e.g., conservation law of the components) [43]. In addition, ‘nonlinearity (or ‘ultrasensitivity’) is required in the positive feedback [33]. Later, we discuss the minimum autocatalytic chemical system that satisfies the above condition.
- [45] A. Blokhuis, D. Lacoste, and P. Gaspard, Reaction kinetics in open reactors and serial transfers between closed reactors, *The Journal of Chemical Physics* **148**, 144902 (2018).
- [46] A. Erez, J. G. Lopez, B. G. Weiner, Y. Meir, and N. S. Wingreen, Nutrient levels and trade-offs control diversity in a serial dilution ecosystem, *Elife* **9**, e57790 (2020).
- [47] N. Vaidya, M. L. Manapat, I. A. Chen, R. Xulvi-Brunet, E. J. Hayden, and N. Lehman, Spontaneous network formation among cooperative rna replicators, *Nature* **491**, 72 (2012).
- [48] J. A. Yeates, C. Hilbe, M. Zwick, M. A. Nowak, and N. Lehman, Dynamics of prebiotic rna reproduction illuminated by chemical game theory, *Proceedings of the National Academy of Sciences* **113**, 5030 (2016).
- [49] Here, we consider the reproduction rate functions are symmetric between  $X_1$  and  $X_2$  for the sake of simplicity. Later we also consider the asymmetric case in the Sec. II E.
- [50] Note that if  $r(x)x$  is monotonic, this is also a necessary condition. However, in general, this is only a sufficient and not necessary condition. For example, there are cases

where both symmetric and asymmetric trajectories are stable if  $r(x)x$  is non-monotonic. For example,  $r(x)x = \epsilon + \kappa x(x^2 - \frac{3}{2}(\alpha + \beta) + 3\alpha\beta)$ .

- [51] S. Arsène, S. Ameta, N. Lehman, A. D. Griffiths, and P. Nghe, Coupled catabolism and anabolism in autocatalytic rna sets, *Nucleic Acids Research* **46**, 9660 (2018).
- [52] The bases M and N are the middle nucleotide of the 3nt recognition element in WXY, called the internal guide sequence (IGS) and the tag sequence [48].
- [53] Here, the background reaction rate is approximated as a constant, although this reaction is due to catalyzed reaction by the non-covalent ribozymes or non-corresponding ribozymes. Assuming that the WXY fragments are abundant, the concentration of non-covalent ribozymes  $WXY:Z$  is  $\sim s$  approximately. We assume their catalytic activity is non-specific, whose reaction rate is  $\epsilon$ . Next, we assume corresponding and non-corresponding ribozymes catalyze at efficiency  $\tilde{\kappa}'$  and  $\tilde{\kappa}$ , respectively. Then, the rate of the reaction  $S \rightarrow X_1$  is  $s\epsilon + x_2\tilde{\kappa}' + x_1\tilde{\kappa}$ . If we assume that  $\epsilon = \tilde{\kappa}'$ , the rate is given as  $\epsilon + \kappa x_1$ , where  $\kappa = \tilde{\kappa}_1 - \epsilon$ .
- [54] Here, the time derivative of difference of concentration between  $X_1$  and  $X_2$  is  $\frac{d}{dt} \left( \frac{\delta}{\chi} \right) = \frac{1}{\chi^2} \left( \frac{d\delta}{dt} \chi - \delta \frac{d\chi}{dt} \right) = -2\epsilon s \frac{\delta}{\chi}$ , where  $\delta = x_1 - x_2$  and  $\chi = x_1 + x_2$ . Therefore,  $\delta/\chi$  decays exponentially into zero in the characteristic relaxation time scale  $\tau = \frac{1}{2s\epsilon}$ . For example, if  $s\epsilon \sim 0.01 \text{ min}^{-1}$ , the half time  $\tau$  is estimated as  $\sim 50 \text{ min}$ .
- [55] The ACSs based on the *Azoarcus* system show slow backward reactions since they are based on the recombination reactions of nucleotides [51].
- [56] Moreover, the *Azoarcus* ribozyme can form cross-catalytic networks [30, 47] (e.g., choosing bases M and N to be CC and GG, or AA and UU); in such cases, each network is a unit of self-reproduction (called an ‘autocatalytic core’) and could compete with other units.
- [57] C. Jeancolas, Y. J. Matsubara, M. Vybornyi, C. N. Lambert, A. Blokhuis, T. Alline, A. D. Griffiths, S. Ameta, S. Krishna, and P. Nghe, Rna diversification by a self-reproducing ribozyme revealed by deep sequencing and kinetic modelling, *Chemical Communications* **57**, 7517 (2021).
- [58] S. Jain and S. Krishna, Crashes, recoveries, and “core shifts” in a model of evolving networks, *Physical Review E* **65**, 026103 (2002).
- [59] K. Kaneko, On recursive production and evolvability of cells: catalytic reaction network approach, *Advanced in Chemical Physics* **130**, 543 (2005).
- [60] This type of bistability: low and high catalyst concentration states, also could appear in our model if the background reaction rate is small enough (nearly zero). However, such bistability is easily destroyed under the SD protocol unless the interval is very short.
- [61] K. Kaneko and T. Yomo, On a kinetic origin of heredity: minority control in a replicating system with mutually catalytic molecules, *Journal of Theoretical Biology* **214**, 563 (2002).
- [62] G. Doucier, A. Lambert, S. De Monte, and P. B. Rainey, Eco-evolutionary dynamics of nested darwinian populations and the emergence of community-level heredity, *Elife* **9**, e53433 (2020).
- [63] N. Takeuchi, N. Mitarai, and K. Kaneko, Scaling laws of multilevel selection: a striking difference between continuous-trait and binary-trait models, arXiv (2020), arXiv:2005.04421.
- [64] S. Matsumura, Á. Kun, M. Ryckelynck, F. Coldren, A. Szilágyi, F. Jossinet, C. Rick, P. Nghe, E. Szathmáry, and A. D. Griffiths, Transient compartmentalization of rna replicators prevents extinction due to parasites, *Science* **354**, 1293 (2016).
- [65] S. Ameta, M. Kumar, N. Chakraborty, Y. J. Matsubara, S. Prashanth, D. Gandavadi, and S. Thutupalli, Multispecies autocatalytic rna reaction networks in coacervates, bioRxiv <https://doi.org/10.1101/2022.11.01.514660> (2022).
- [66] W. H. Press, S. A. Teukolsky, W. T. Vetterling, and B. P. Flannery, *Numerical recipes 3rd edition: The art of scientific computing* (Cambridge university press, 2007).
- [67] B. Shirt-Ediss, R. V. Solé, and K. Ruiz-Mirazo, Emergent chemical behavior in variable-volume protocells, *Life* **5**, 181 (2015).
- [68] T. Ruiz-Herrero, T. G. Fai, and L. Mahadevan, Dynamics of growth and form in prebiotic vesicles, *Physical review letters* **123**, 038102 (2019).
- [69] P. L. Luisi, Enzymes hosted in reverse micelles in hydrocarbon solution, *Angewandte Chemie International Edition* **24**, 439 (1985).
- [70] P. L. Luisi and F. J. Varela, Self-replicating micelles—a chemical version of a minimal autopoietic system, *Origins of Life and Evolution of the Biosphere* **19**, 633 (1989).
- [71] C. W. Gardiner *et al.*, *Handbook of stochastic methods*, Vol. 3 (springer Berlin, 1985).
- [72] D. T. Gillespie, The chemical langevin equation, *The Journal of Chemical Physics* **113**, 297 (2000).
- [73] The dilution factor  $m$  could also be randomly distributed, or depending on the random variable interval at each cycle  $\Delta t$ . In these cases, the results do not qualitatively differ.

## Appendix A: Inheritable variety in general autocatalytic systems

### 1. The necessary condition under the serial dilution protocol

We consider the competing autocatalytic entities,  $X_1$  and  $X_2$ , under the SD protocol. The rate equation for the concentration for the entities,  $x_1$  and  $x_2$ , during one cycle until the dilution, are Eq. 1 in the main text,

$$\frac{dx_i}{dt} = s(\{x_j\}, t)r(x_i)x_i, \quad (S1)$$

where  $s(\{x_j\}, t)$  is the concentration of the substrate  $S$  that is consumed in the replication reactions and  $r(x_i)$  is the reproduction rate of  $x_i$ , respectively. Here we assume  $s$  is symmetrical under exchange of  $x_i$ s, i.e.,  $s(x_1, x_2) = s(x_2, x_1)$  and  $s, x_i$ s satisfy some conservation law (e.g.,  $s + x_1 + x_2 = s^{tot}$ ). Also, we assume  $s$  and  $r$  are differentiable and non-negative functions for  $x_1 \geq 0$  and  $x_2 \geq 0$ .

Here, we define  $\chi = x_1 + x_2$  and  $\delta = x_1 - x_2$ , respectively. Then, the time derivative of them are

$$\frac{d\chi}{dt} = sr\left(\frac{\chi}{2}\right)\chi + \mathcal{O}(\delta^2), \quad \frac{d\delta}{dt} = s\left(r\left(\frac{\chi}{2}\right) + \frac{1}{2}\chi\frac{dr}{d\chi}\left(\frac{\chi}{2}\right)\right)\delta + \mathcal{O}(\delta^2), \quad (S2)$$

where we used the expansion  $r\left(\frac{1}{2}(\chi \pm \delta)\right) = r\left(\frac{\chi}{2}\right) \pm \frac{dr}{d\chi}\left(\frac{\chi}{2}\right)\frac{\delta}{2} + \mathcal{O}\left(\left(\frac{\delta}{2}\right)^2\right)$ , and assumed  $\delta$  is small compared with  $\chi$ , i.e., the concentrations of two catalysts are nearly equal,  $x_1 \sim x_2$ . Then,

$$\frac{d}{dt}\left(\frac{\delta}{\chi}\right) = \frac{1}{\chi^2}\left(\frac{d\delta}{dt}\chi - \frac{d\chi}{dt}\delta\right) = s\left(\frac{1}{2}\frac{dr}{d\chi}\left(\frac{\chi}{2}\right)\chi\right)\frac{\delta}{\chi}. \quad (S3)$$

The integration of  $\frac{d}{dt}\left(\frac{\delta}{\chi}\right)/\left(\frac{\delta}{\chi}\right)$  lead to

$$\begin{aligned} \log\left|\frac{\delta(t)}{\chi(t)}\right| &= \int_0^t \frac{1}{2}s\frac{dr}{d\chi}\left(\frac{\chi}{2}\right)\chi dt + \log\left|\frac{\delta(0)}{\chi(0)}\right| \\ &= \int_{\chi(0)}^{\chi(t)} \frac{dr}{r(x)} dx + \log\left|\frac{\delta(0)}{\chi(0)}\right|, \end{aligned} \quad (S4)$$

where we used  $\frac{dt}{d\chi} = 1/(sr(\frac{\chi}{2})\chi)$ . Therefore,

$$\frac{\delta(t)}{\chi(t)} = \frac{r\left(\frac{\chi(t)}{2}\right)}{r\left(\frac{\chi(0)}{2}\right)}\frac{\delta(0)}{\chi(0)}, \quad (S5)$$

which is Eq. 2 in the main text.

Now, we consider the serial dilution protocol, i.e., the amounts of  $x_1$  and  $x_2$  are multiplied by  $m^{-1}$  at the end of a cycle  $t = \Delta t$ . In the stationary trajectory,  $\chi(t)$  should satisfy the condition  $\chi(\Delta t) = m\chi(0)$ . If the condition

$$\frac{\delta(\Delta t)}{\chi(\Delta t)} > \frac{\delta(0)}{\chi(0)} \quad (S6)$$

is met, the difference between  $x_1$  and  $x_2$ ,  $\delta/\chi$  is magnified during a cycle. Therefore, the stationary trajectory with the equal concentration of  $X_1$  and  $X_2$  (i.e.,  $\delta = 0$ ) is unstable; if otherwise, the stationary trajectory is stable.

Thus, surprisingly, whether the trajectory is stable or not is determined by only whether the replication rate at the end of a cycle  $r\left(\frac{\chi(\Delta t)}{2}\right)$  is larger than that at the beginning  $r\left(\frac{\chi(0)}{2}\right)$  or not. Roughly, the replication rates at the beginning and the end are interpreted as the background and catalyzed reaction rates. For example, if  $r(x) = \frac{\epsilon + \kappa x}{x}$  (the system based on the *Azoarcus* ribozyme) the stationary trajectory with  $\delta = 0$  is always stable. If  $r(x) = \frac{(\epsilon + \kappa x)^2}{x}$ ,  $\Delta t_c$  is calculated as  $\Delta t_c = \log\left|\frac{\epsilon + \kappa s^{tot}}{\epsilon + \kappa s^{tot}m^{-1}}\right|^2 \sim 2\log\left(1 + \frac{\kappa s^{tot}}{\epsilon}\right)$ .

### 2. The necessary condition for the heredity under the CSTR

Next, we consider the competing autocatalytic systems under the CSTR condition, where the constant dilution rate is  $\bar{\phi}$ . Similar as in the previous section, the rate equations for  $x_1$  and  $x_2$  are

$$\frac{dx_i}{dt} = s(\{x_j\}, t)r(x_i)x_i - \bar{\phi}x_i, \quad (S7)$$

where the notations are the same as in the previous section.

Here, the time derivative of  $\chi$  and  $\delta$  ( $\chi = x_1 + x_2$  and  $\delta = x_1 - x_2$ ) are

$$\frac{d\chi}{dt} = sr\left(\frac{\chi}{2}\right)\chi - \bar{\phi}\chi + \mathcal{O}(\delta^2), \quad \frac{d\delta}{dt} = s\left(r\left(\frac{\chi}{2}\right) + \frac{1}{2}\chi\frac{dr}{d\chi}\left(\frac{\chi}{2}\right)\right)\delta - \bar{\phi}\delta + \mathcal{O}(\delta^2), \quad (\text{S8})$$

where we used  $r\left(\frac{1}{2}(\chi \pm \delta)\right) = r\left(\frac{\chi}{2}\right) \pm \frac{dr}{d\chi}\left(\frac{\chi}{2}\right)\frac{\delta}{2} + \mathcal{O}\left(\left(\frac{\delta}{2}\right)^2\right)$ , and assumed  $\delta$  is small. The same calculation in the previous section leads to

$$\frac{d}{dt}\left(\frac{\delta}{\chi}\right) = \frac{1}{\chi^2}\left(\frac{d\delta}{dt}\chi - \frac{d\chi}{dt}\delta\right) = s\left(\frac{1}{2}\frac{dr}{d\chi}\left(\frac{\chi}{2}\right)\chi\right)\frac{\delta}{\chi} + \mathcal{O}\left((\delta/\chi)^2\right). \quad (\text{S9})$$

Thus, given the steady state concentration  $\chi^*$  such that  $s^*r\left(\frac{\chi^*}{2}\right) = \bar{\phi}$ , the state with  $\delta = 0$  is stable if  $\frac{dr}{d\chi}\left(\frac{\chi^*}{2}\right)$  is negative. For example, if  $r(x) = \frac{\epsilon + \kappa x}{x}$  (the *Azoarcus* based system with only one step),  $\frac{dr}{d\chi}(x) = -\epsilon/x^2$  is negative for all  $x$ , therefore the state with  $\delta = 0$  is always stable. While in a case with  $r(x) = \frac{\epsilon + \kappa x^2}{x}$ ,  $\frac{dr}{d\chi}(x) = -\epsilon/x^2 + \kappa$ . Therefore, if  $\bar{\phi} > \phi_c^{cstr}$ , where  $\phi_c^{cstr} = s^{tot}\sqrt{\epsilon\kappa} - 4\epsilon$ , the state with  $\delta = 0$  is stable.

Note that, for the stability of the steady state  $\chi^*$ , the condition  $-r\left(\frac{\chi^*}{2}\right) + \frac{1}{2}(s^{tot} - \chi^*)\frac{dr}{d\chi}\left(\frac{\chi^*}{2}\right) < 0$  should be satisfied. The  $\chi$ -direction is always stable if  $\delta$ -direction is stable, i.e.,  $\frac{dr}{d\chi}\left(\frac{\chi^*}{2}\right) < 0$ .

### 3. Under the general dilution protocol (compartment growth and division)

Lastly, we discuss the heredity of the system under the general dilution scenarios:

$$\frac{dx_i}{dt} = s(\{x_j\}, t)r(x_i)x_i - \phi(t)x_i, \quad (\text{S10})$$

where  $\phi(t)$  is the time-dependent dilution rate due to the growth of the compartment volume  $V$ ,  $\phi(t) = \frac{dV}{dt}/V$ . Here we restrict  $\phi(t)$  to periodic functions  $\phi(t + \Delta t) = \phi(t)$  such that  $\int_0^{\Delta t} \phi(t)dt = \bar{\phi}\Delta t$ . Also  $\sigma(t) = s^{tot}\phi(t)$ , thus the total mass of the substrate is kept as a constant,  $s + \sum_i x_i = s^{tot}$ . We further assume that  $r(x)$  is a convex function, i.e.,  $\frac{d^2r}{dx^2}(x) > 0$ .

Under the above setup, the critical interval  $\Delta t_c$ , which divides the region with and without heredity, is bounded by both that under the serial dilution and the CSTR:

1. The period  $\Delta t_c$  for the protocol under any  $\phi(t)$  is bounded from the above by that under the CSTR  $\Delta t_c^{cstr}$ ,  $\Delta t_c \leq \Delta t_c^{cstr}$ . Here,  $\Delta t_c^{cstr}$  is either  $\infty$  or 0.
2.  $\Delta t_c$  is bounded from the bottom by that under the serial dilution  $\Delta t_c^{sd}$ ,  $\Delta t_c^{sd} \leq \Delta t_c$ .

To prove this (non-rigorously), we use the dilution rate function  $\phi(t)$

$$\phi(t) \equiv \begin{cases} \bar{\phi}_1 & (0 \leq t \leq \tau), \\ \bar{\phi}_2 & (\tau \leq t \leq \Delta t). \end{cases} \quad (\text{S11})$$

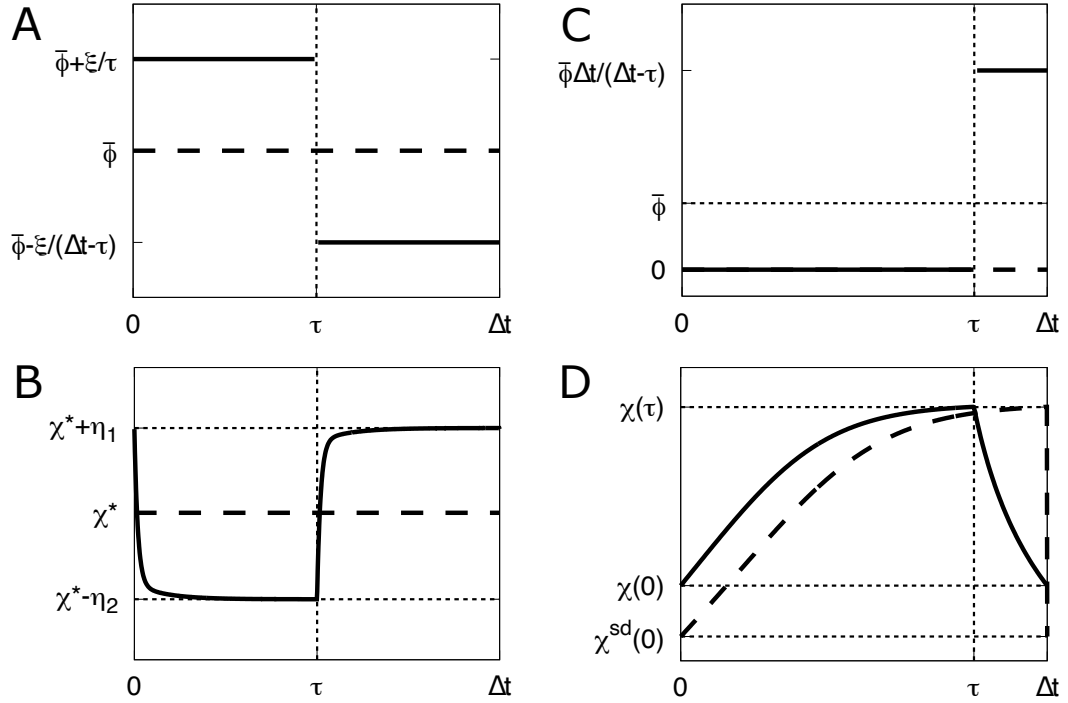


FIG. S1. Schematics for the proof in Sec. A 3. Left figures represent the time-dependent dilution rate in one dilution cycle,  $\phi(t)$ , and right figures represent  $\chi(t)$ . The top figures are for the perturbation from the CSTR condition (The dashed lines represent the corresponding case under the CSTR condition). The bottom figures are for the perturbation from the SD condition (The dashed lines represent the corresponding SD).

*a. The perturbation from the CSTR condition:* Firstly, we consider the perturbation from the CSTR protocol fixing  $\int_0^{\Delta t} \phi(t) dt = \bar{\phi} \Delta t$ , i.e.,  $\bar{\phi}_1 = \bar{\phi} + \frac{\xi}{\tau}$  and  $\bar{\phi}_2 = \bar{\phi} - \frac{\xi}{\Delta t - \tau}$  (see Fig. S1). Here, we define the steady-state concentration under the CSTR with the constant dilution rate  $\bar{\phi}$ ,  $\chi^*$ , is such that  $(s^{tot} - \chi^*)r(\chi^*)\chi^* - \bar{\phi} = 0$ . Here we consider a small perturbation for  $\bar{\phi}$ ,  $\bar{\phi} \rightarrow \bar{\phi} + \xi_i$ , where  $\xi_1 = \frac{\xi}{\tau}$  and  $\xi_2 = -\frac{\xi}{\Delta t - \tau}$ , and the deviation for  $\chi^*$  due to it,  $\chi^* \rightarrow \chi^* + \eta_i$ , which should satisfies

$$\begin{aligned}
 (s^{tot} - \chi^* - \eta_i)r\left(\frac{\chi^* + \eta_i}{2}\right) - (\bar{\phi} + \xi_i) &= 0, \\
 (s^{tot} - \chi^* - \eta_i)\left(r\left(\frac{\chi^*}{2}\right) + \frac{\eta_i}{2}\frac{dr}{dx}\left(\frac{\chi^*}{2}\right) + \frac{\eta_i^2}{8}\frac{d^2r}{dx^2}\left(\frac{\chi^*}{2}\right) + \mathcal{O}(\eta_i^3)\right) - (\bar{\phi} + \xi_i) &= 0, \quad (S12) \\
 \eta_i\left(-r\left(\frac{\chi^*}{2}\right) + (s^{tot} - \chi^*)\frac{1}{2}\frac{dr}{dx}\left(\frac{\chi^*}{2}\right)\right) + \eta_i^2\left(-\frac{1}{2}\frac{dr}{dx}\left(\frac{\chi^*}{2}\right) + (s^{tot} - \chi^*)\frac{1}{8}\frac{d^2r}{dx^2}\left(\frac{\chi^*}{2}\right)\right) + \mathcal{O}(\eta_i^3) - \xi_i &= 0,
 \end{aligned}$$

where we used the expansion  $r\left(\frac{\chi^* + \eta_i}{2}\right) = r\left(\frac{\chi^*}{2}\right) + \frac{\eta_i}{2}\frac{dr}{dx}\left(\frac{\chi^*}{2}\right) + \frac{\eta_i^2}{8}\frac{d^2r}{dx^2}\left(\frac{\chi^*}{2}\right) + \mathcal{O}(\eta_i^3)$ , and  $(s^{tot} - \chi^*)r(\chi^*) - \bar{\phi} = 0$ . Then,  $\eta_i$  is determined as

$$\eta_i = -\tilde{\xi}_i - \frac{1}{2}\mathcal{R}\tilde{\xi}_i^2 + \mathcal{O}(\xi_i^3), \quad (S13)$$

where we define

$$\tilde{\xi}_i = \frac{\xi_i}{r\left(\frac{\chi^*}{2}\right) - \frac{1}{2}(s^{tot} - \chi^*)\frac{dr}{dx}\left(\frac{\chi^*}{2}\right)}, \quad \mathcal{R} = \frac{\frac{dr}{dx}\left(\frac{\chi^*}{2}\right) - \frac{1}{4}(s^{tot} - \chi^*)\frac{d^2r}{dx^2}\left(\frac{\chi^*}{2}\right)}{r\left(\frac{\chi^*}{2}\right) - \frac{1}{2}(s^{tot} - \chi^*)\frac{dr}{dx}\left(\frac{\chi^*}{2}\right)}. \quad (S14)$$

Note that, from the condition for the stability of the steady state  $\chi^*$ ,  $\frac{d}{dt}((s^{tot} - x)r(\frac{x}{2}) - \bar{\phi})|_{x=\chi^*} < 0$ ,  $\frac{1}{2}(s^{tot} - \chi^*)\frac{dr}{dx}\left(\frac{\chi^*}{2}\right) - r\left(\frac{\chi^*}{2}\right) < 0$ .



The same as the previous sections, the integration of  $\frac{d}{dt}\left(\frac{\delta}{\chi}\right)/\left(\frac{\delta}{\chi}\right)$  from  $t = 0$  to  $= \Delta t$  lead to

$$\begin{aligned} \log \left| \frac{\delta(\Delta t)}{\chi(\Delta t)} \right| - \log \left| \frac{\delta(0)}{\chi(0)} \right| &= \frac{1}{2} \int_0^{\Delta t} (s^{tot} - \chi) \chi \frac{dr}{dx} \left( \frac{\chi}{2} \right) dt, \\ &\approx \tau (s^{tot} - \chi^* - \eta_1) \frac{\chi^* + \eta_1}{2} \frac{dr}{dx} \left( \frac{\chi^* + \eta_1}{2} \right) + (\Delta t - \tau) (s^{tot} - \chi^* - \eta_2) \frac{\chi^* + \eta_2}{2} \frac{dr}{dx} \left( \frac{\chi^* + \eta_2}{2} \right), \end{aligned} \quad (\text{S15})$$

where we assumed that when  $\phi$  is changed (at  $t = 0$  and  $t = \tau$ ), the relaxation time to the steady concentration is much smaller than  $\tau$  and  $\Delta t - \tau$  (see Fig. S1), whose contribution is of the order of  $\xi^3$ . Then, substituting Eq. S13 into the above,

$$\begin{aligned} &= \Delta t (s^{tot} - \chi^*) \frac{\chi^*}{2} \frac{dr}{dx} \left( \frac{\chi^*}{2} \right) \\ &\quad + (\tau \eta_1 + (\Delta t - \tau) \eta_2) \left( \left( \frac{1}{2} s^{tot} - \chi^* \right) \frac{dr}{dx} \left( \frac{\chi^*}{2} \right) + (s^{tot} - \chi^*) \frac{\chi^*}{4} \frac{d^2 r}{dx^2} \left( \frac{\chi^*}{2} \right) \right) \\ &\quad + (\tau \eta_1^2 + (\Delta t - \tau) \eta_2^2) \left( \left( s^{tot} - 2\chi^* \right) \frac{1}{4} \frac{d^2 r}{dx^2} \left( \frac{\chi^*}{2} \right) - \frac{1}{2} \frac{dr}{dx} \left( \frac{\chi^*}{2} \right) + (s^{tot} - \chi^*) \frac{\chi^*}{16} \frac{d^3 r}{dx^3} \left( \frac{\chi^*}{2} \right) \right) + \mathcal{O}(\xi^3), \\ &= \Delta t (s^{tot} - \chi^*) \frac{\chi^*}{2} \frac{dr}{dx} \left( \frac{\chi^*}{2} \right) - \frac{1}{2} \xi^2 \left( \frac{1}{\tau} + \frac{1}{\Delta t - \tau} \right) \left[ \mathcal{R} \left( \left( \frac{1}{2} s^{tot} - \chi^* \right) \frac{dr}{dx} \left( \frac{\chi^*}{2} \right) + (s^{tot} - \chi^*) \frac{\chi^*}{4} \frac{d^2 r}{dx^2} \left( \frac{\chi^*}{2} \right) \right) \right. \\ &\quad \left. + \left( \chi^* - \frac{1}{2} s^{tot} \right) \frac{d^2 r}{dx^2} \left( \frac{\chi^*}{2} \right) + \frac{dr}{dx} \left( \frac{\chi^*}{2} \right) - (s^{tot} - \chi^*) \frac{\chi^*}{8} \frac{d^3 r}{dx^3} \left( \frac{\chi^*}{2} \right) \right] + \mathcal{O}(\xi^3), \end{aligned} \quad (\text{S16})$$

where the first term is the deviation under the CSTR with the dilution rate  $\bar{\phi}$ ,  $\log \left[ \frac{\delta^{cstr}(\Delta t)}{\chi^{cstr}(\Delta t)} / \frac{\delta^{cstr}(0)}{\chi^{cstr}(0)} \right]$ . When  $\frac{dr}{dx} \left( \frac{\chi^*}{2} \right) = 0$ ,

$$= -\frac{1}{2} \xi^2 \left( \frac{1}{\tau} + \frac{1}{\Delta t - \tau} \right) \left( \left( \chi^* - \frac{1}{2} s^{tot} \right) \frac{d^2 r}{dx^2} \left( \frac{\chi^*}{2} \right) - \frac{1}{16} (s^{tot} - \chi^*)^2 \chi^* \frac{\left( \frac{d^2 r}{dx^2} \left( \frac{\chi^*}{2} \right) \right)^2}{r \left( \frac{\chi^*}{2} \right)} - \frac{1}{8} (s^{tot} - \chi^*) \chi^* \frac{d^3 r}{dx^3} \left( \frac{\chi^*}{2} \right) \right) + \mathcal{O}(\xi^3). \quad (\text{S17})$$

Here, if we approximate that  $\chi^*$  is nearly saturated, i.e.,  $\chi^* \sim s^{tot}$ ,

$$\sim -\frac{1}{4} \xi^2 \left( \frac{1}{\tau} + \frac{1}{\Delta t - \tau} \right) s^{tot} \frac{d^2 r}{dx^2} \left( \frac{\chi^*}{2} \right) + \mathcal{O}(\xi^3). \quad (\text{S18})$$

Therefore, under the  $\phi(t)$  with any choice of  $\xi$  and  $\tau$ ,  $\frac{\delta(\Delta t)}{\chi(\Delta t)} / \frac{\delta(0)}{\chi(0)} < \frac{\delta^{cstr}(\Delta t)}{\chi^{cstr}(\Delta t)} / \frac{\delta^{cstr}(0)}{\chi^{cstr}(0)}$ . Thus, if the stationary trajectory with  $\delta = 0$  is stable under the CSTR, i.e.,  $\frac{\delta^{cstr}(\Delta t)}{\chi^{cstr}(\Delta t)} / \frac{\delta^{cstr}(0)}{\chi^{cstr}(0)} < 1$ , it is also true for that under the protocol with the dilution rate  $\phi(t)$ , therefore,  $\Delta t_c \leq \Delta t_c^{cstr}$ .

Further, we can divide the region for  $\bar{\phi}_1$  or  $\bar{\phi}_2$ , and add more steps for the function  $\phi(t)$ . The same analysis as the above reveals that in each addition  $\frac{\delta(\Delta t)}{\chi(\Delta t)} / \frac{\delta(0)}{\chi(0)}$  declines monotonically, thus the upper limit for heredity  $\Delta t_c$  also declines monotonically.

*b. The perturbation from the serial dilution protocol:* Secondly, we also consider the perturbation from the case with the serial dilution; here we consider  $\bar{\phi}_1$  and  $\bar{\phi}_2$  as  $\bar{\phi}_1 = 0$  and  $\bar{\phi}_2 = \bar{\phi} \frac{\Delta t}{\Delta t - \tau}$  (see Fig. S1). Note that when  $\Delta t - \tau \rightarrow 0$ , the dilution protocol becomes the same as the serial dilution.

The deviation of  $\frac{\delta}{\chi}$  in one cycle under the dilution protocol with  $\phi(t)$ ,

$$\begin{aligned} \log \left| \frac{\delta(\Delta t)}{\chi(\Delta t)} \right| - \log \left| \frac{\delta(0)}{\chi(0)} \right| &= \frac{1}{2} \int_0^{\Delta t} (s^{tot} - \chi) \chi \frac{dr}{dx} \left( \frac{\chi}{2} \right) dt, \\ &= \int_{\frac{\chi(0)}{2}}^{\frac{\chi(\tau)}{2}} \frac{dr}{r} dx + \frac{1}{2} \int_{\tau}^{\Delta t} (s^{tot} - \chi) \chi \frac{dr}{dx} \left( \frac{\chi}{2} \right) dt \end{aligned} \quad (\text{S19})$$

We assume  $\chi^{sd}(\Delta t) \sim \chi(\tau)$ , because in the both cases  $\chi(t)$  is saturated (i.e., S is exhausted) if  $\Delta t$  is enough large

(see Fig. S1). Then,  $\chi^{sd}(0) = \chi(\tau) \exp(-\bar{\phi}\Delta t)$ . From the rate equation  $\frac{d\chi}{dt} = ((s^{tot} - \chi)r(\frac{\chi}{2}) - \bar{\phi})\chi$

$$\begin{aligned}\chi(\Delta t) &= \chi(0) = \chi(\tau) \exp\left(-\Delta t\bar{\phi} + \int_{\tau}^{\Delta t} (s^{tot} - \chi)r\left(\frac{\chi}{2}\right) dt\right), \\ &= \chi^{sd}(0) \exp\left(\int_{\tau}^{\Delta t} (s^{tot} - \chi)r\left(\frac{\chi}{2}\right) dt\right).\end{aligned}\tag{S20}$$

On the other hand, the deviation of  $\frac{\delta^{sd}}{\chi^{sd}}$  in one cycle under SD is derived as

$$\log\left|\frac{\delta^{sd}(\Delta t)}{\chi^{sd}(\Delta t)}\right| - \log\left|\frac{\delta^{sd}(0)}{\chi^{sd}(0)}\right| = \int_{\frac{\chi^{sd}(0)}{2}}^{\frac{\chi(0)}{2}} \frac{dr}{r} dx + \int_{\frac{\chi(0)}{2}}^{\frac{\chi(\tau)}{2}} \frac{dr}{r} dx,\tag{S21}$$

Here, the first term is,

$$\int_{\frac{\chi^{sd}(0)}{2}}^{\frac{\chi(0)}{2}} \frac{dr}{r} dx = \log\left|\frac{r\left(\frac{\chi(0)}{2}\right)}{r\left(\frac{\chi^{sd}(0)}{2}\right)}\right| = \frac{\chi^{sd}(0)}{2} \frac{dr\left(\frac{\chi^{sd}(0)}{2}\right)}{r\left(\frac{\chi^{sd}(0)}{2}\right)} \int_{\tau}^{\Delta t} (s^{tot} - \chi)r\left(\frac{\chi}{2}\right) dt + \mathcal{O}((\Delta t - \tau)^2),\tag{S22}$$

where in the approximation, we used the assumption that  $\Delta t - \tau$  is small.

From the comparison between Eq. S21 Eq. S19,

$$\begin{aligned}&\log\left|\frac{\delta(\Delta t)}{\chi(\Delta t)}\right| - \log\left|\frac{\delta(0)}{\chi(0)}\right| - \left(\log\left|\frac{\delta^{sd}(\Delta t)}{\chi^{sd}(\Delta t)}\right| - \log\left|\frac{\delta^{sd}(0)}{\chi^{sd}(0)}\right|\right) \\ &= \frac{1}{2} \int_{\tau}^{\Delta t} (s^{tot} - \chi(t')) \left[ \chi(t') \frac{dr}{dx}\left(\frac{\chi(t')}{2}\right) - \frac{r\left(\frac{\chi(t')}{2}\right) \chi^{sd}(0) \frac{dr}{dx}\left(\frac{\chi^{sd}(0)}{2}\right)}{r\left(\frac{\chi^{sd}(0)}{2}\right)} \right] dt'.\end{aligned}\tag{S23}$$

Thus, if  $\frac{\chi(t) \frac{dr}{dx}\left(\frac{\chi(t)}{2}\right)}{r\left(\frac{\chi(t)}{2}\right)} > \frac{\chi^{sd}(0) \frac{dr}{dx}\left(\frac{\chi^{sd}(0)}{2}\right)}{r\left(\frac{\chi^{sd}(0)}{2}\right)}$  is satisfied, the above is always positive. As  $\chi(t) > \chi^{sd}(0)$ , it reveals that  $\frac{\delta(\Delta t)}{\chi(\Delta t)} / \frac{\delta(0)}{\chi(0)} > \frac{\delta^{sd}(\Delta t)}{\chi^{sd}(\Delta t)} / \frac{\delta^{sd}(0)}{\chi^{sd}(0)}$  for the serial dilution is always less than that for the protocol with the dilution rate function  $\phi(t)$ , if  $\frac{x \frac{dr}{dx}(x)}{r(x)}$  is an increasing function of  $x$ . Therefore, the critical period of time for  $\phi(t)$ ,  $\Delta t_c$  is always larger than that for the serial dilution,  $\Delta t_c^{sd}$ , i.e.,  $\Delta t_c^{sd} \leq \Delta t_c$ .

## Appendix B: robustness of results

### 1. Autocatalytic sets with reversible chemical reactions

In the main text, we mainly considered chemical reaction systems with irreversible reactions. However, all reactions should be reversible to be chemically consistent and converge to thermal equilibrium in the absence of dilution protocols. Here, we expand our previous analysis to examine how reversible reactions change the phase diagram of bistability.

If the reactions in the system in Fig. 3A is reversible, the rate equations are

$$\frac{dx_i}{dt} = (s - bx_i)r(x_i)x_i,\tag{S1}$$

where  $b$  is the relative rate of the backward reaction (see Fig. S2).

Then,  $\frac{d\chi}{dt}$  and  $\frac{d\delta}{dt}$  are modified as

$$\begin{aligned}\frac{d\chi}{dt} &= (s - \frac{b}{2}\chi)r\left(\frac{\chi}{2}\right)\chi + \mathcal{O}(\delta^2), \\ \frac{d\delta}{dt} &= s\left(r\left(\frac{\chi}{2}\right) + \frac{1}{2}\chi \frac{dr}{dt}\left(\frac{\chi}{2}\right)\right)\delta - b\left(r\left(\frac{\chi}{2}\right) + \frac{1}{4}\chi \frac{dr}{dt}\left(\frac{\chi}{2}\right)\right)\chi\delta + \mathcal{O}(\delta^2).\end{aligned}\tag{S2}$$

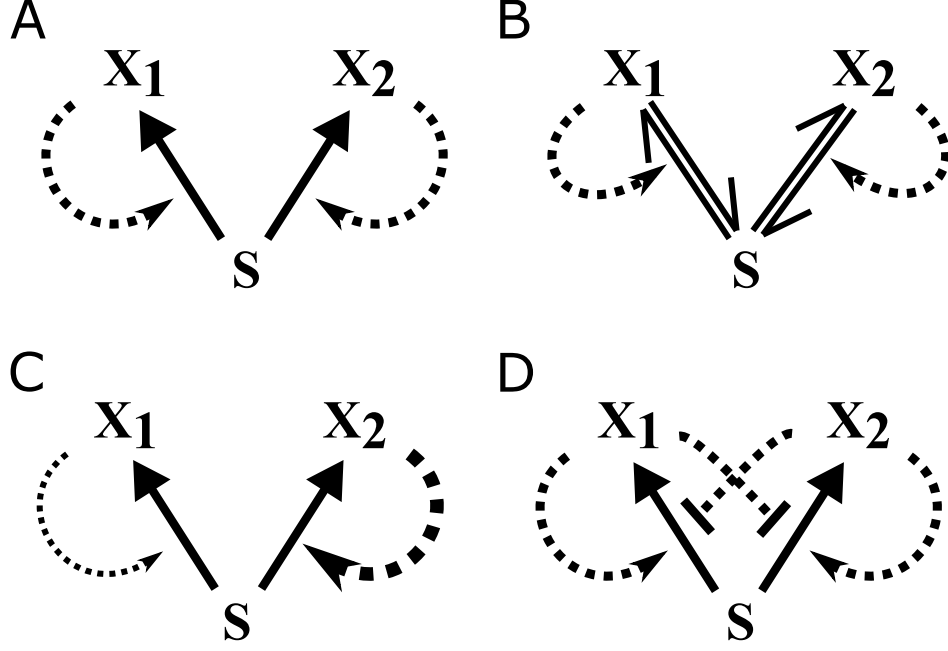


FIG. S2. Schematics of the alternative models for the competing autocatalytic entities,  $X_1$  and  $X_2$ ; they are converted from a substrate  $S$  (solid arrows) catalyzed by itself (dashed arrows). (A) non-modified model (the same as Fig. 3A in the main text) (B) with reversible chemical reactions (Sec. B 1) (C) with asymmetric kinetics rates (Sec. B 2) (D) with more general reproduction rate function (dashed arrow with bar head represents the inhibition; Sec. B 3)

Then,

$$\frac{d}{dt}\left(\frac{\delta}{\chi}\right) = \left[ \left(s - \frac{b}{2}\chi\right) \left(\frac{1}{2} \frac{dr}{dt}\left(\frac{\chi}{2}\right)\chi\right) - \frac{1}{2}b\left(r\left(\frac{\chi}{2}\right)\chi\right) \right] \frac{\delta}{\chi}. \quad (\text{S3})$$

As a result,

$$\log \left| \frac{\delta(t)}{\chi(t)} \right| = \left[ \log(r(x)) + \frac{b}{2+b} \log(s^{tot} - (2+b)x) \right]_{x=\frac{\chi(0)}{2}}^{x=\frac{\chi(t)}{2}} + \log \left| \frac{\delta(0)}{\chi(0)} \right|, \quad (\text{S4})$$

where we used  $s = s^{tot} - \chi$ . Thus, the reversible reactions alter Eq. 2 in the main text as

$$\frac{\delta(t)}{\chi(t)} = \frac{r\left(\frac{\chi(t)}{2}\right)}{r\left(\frac{\chi(0)}{2}\right)} \left( \frac{s^{tot} - (1 + \frac{b}{2})\chi(t)}{s^{tot} - (1 + \frac{b}{2})\chi(0)} \right)^{\frac{b}{2+b}} \frac{\delta(0)}{\chi(0)}. \quad (\text{S5})$$

Note that, from Eq. S2,  $s^{tot} - (1 + \frac{b}{2})\chi(\infty) = 0$  at the equilibrium, thus  $\frac{\delta(t)}{\chi(t)}$  eventually converges to 0.

Similar to the case with irreversible reaction ( $b = 0$ ) in the main text, the system shows bifurcation that the bistability disappears when varying the cycle interval  $\Delta t$  or the dilution rate  $\bar{\phi}$ . Interestingly, unlike the irreversible reaction case ( $b = 0$ ), the region of bistability is bounded in the reversible case ( $b > 0$ ) for the parameter  $\bar{\phi}$ . Thus, for the SD protocol with fixed  $\Delta t$ , there is both an upper and a lower critical  $\bar{\phi}$  (see Fig. S3). Note that the boundary of the region is close to the irreversible case when  $\bar{\phi}$  is large and the critical value depends on  $\epsilon$  similarly to the  $b = 0$  case. Importantly, even with reversible reactions, the parameter space for the general GD protocol contains that for SD protocols, as we found for irreversible reactions.

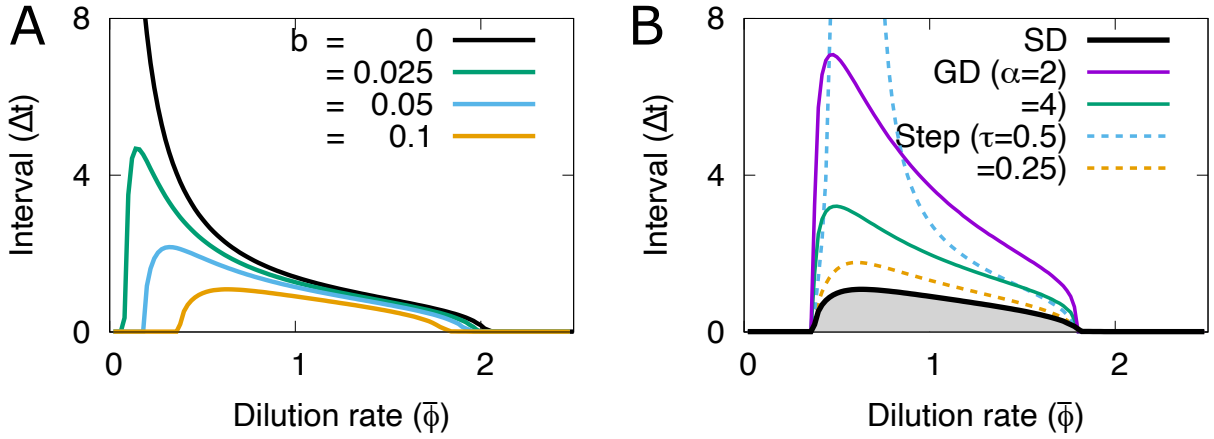


FIG. S3. Phase space of the bistability in the case with reversible reactions (Eq. S2). (A) The colored lines represent the boundary between with or without bistability in different backward reaction rates  $b$ . The other parameters are set as  $\epsilon = 0.5$ ,  $\kappa = 8$  and  $\bar{\phi} = 1$ . (B) The boundary between with or without bistability under various functions of the dilution rates  $\phi(t)$ . We set  $b = 0.1$ .

## 2. ACSs with asymmetric kinetic rates

In the previous sections, we considered symmetric competing ACSs. However, our results are similar even if the two competing ACSs have different kinetic rate constants (catalytic efficiency), although the bifurcation where the bistability disappears is discontinuous.

In Eq. 1 in the main text, we assumed the reproduction rate function,  $r(x_i)$  is the same between the two self-reproducing entities. Here, we also discuss the rate functions of two entities,  $r_1(x_1)$  and  $r_2(x_2)$  are different, i.e.,  $r_1(x) \neq r_2(x)$ . The simplest example is  $r_i(x)x = \epsilon + \kappa_i x^2$ , where  $\kappa_1 \neq \kappa_2$ . In this case, if the difference between the catalytic strength of two entities  $|\kappa_1 - \kappa_2|$  is not so large, the system has the bistability, as the nullclines shows (Fig. S4A). Further, as the bifurcation diagram shows (Fig. S4B), even in this case, the critical point for the interval  $\Delta t$  and the dilution rate  $\bar{\phi}$  exist, although the transition is discontinuous.

In such cases, the boundary in the parameter space for ACSs that have bistability in the general GD protocols is also bounded by the boundaries for the SD and CSTR protocols.

## 3. More general reproduction rate function

Here, we consider the autocatalytic system is under the SD protocol, in which the reproduction rate function depends on both  $x_1$  and  $x_2$ , including cases where  $X_1$  and  $X_2$  mutually inhibit their synthesis (see Fig. S2D). For example, in the case of the genetic toggle switch model [32],  $r(x_i, x_{-i}) = \frac{1}{x_i} \left( \frac{1}{1+x_i^n} \right)$ , where  $n$  is the Hill coefficient.

The rate equations are

$$\frac{dx_i}{dt} = sr(x_i, x_{-i})x_i. \quad (\text{S6})$$

where  $-i$  represents 2 or 1, if  $i = 1$  or 2, respectively.

Here, the same as before, we define  $\chi = x_1 + x_2$ ,  $\delta = x_1 - x_2$ , then

$$\frac{d\chi}{dt} = sr\left(\frac{\chi}{2}, \frac{\chi}{2}\right)\chi + \mathcal{O}(\delta^2), \quad \frac{d\delta}{dt} = s \left( r\left(\frac{\chi}{2}, \frac{\chi}{2}\right) + \frac{1}{2}\chi \frac{\partial r}{\partial x_i}\left(\frac{\chi}{2}, \frac{\chi}{2}\right) - \frac{1}{2}\chi \frac{\partial r}{\partial x_{-i}}\left(\frac{\chi}{2}, \frac{\chi}{2}\right) \right) \delta + \mathcal{O}(\delta^2), \quad (\text{S7})$$

where we used the expansion

$$r\left(\frac{1}{2}(\chi \pm \delta), \frac{1}{2}(\chi \mp \delta)\right) = r\left(\frac{\chi}{2}, \frac{\chi}{2}\right) \pm \frac{\partial r}{\partial x_i}\left(\frac{\chi}{2}, \frac{\chi}{2}\right) \frac{\delta}{2} \mp \frac{\partial r}{\partial x_{-i}}\left(\frac{\chi}{2}, \frac{\chi}{2}\right) \frac{\delta}{2} + \mathcal{O}(\delta^2),$$

and assumed  $\delta$  is small.

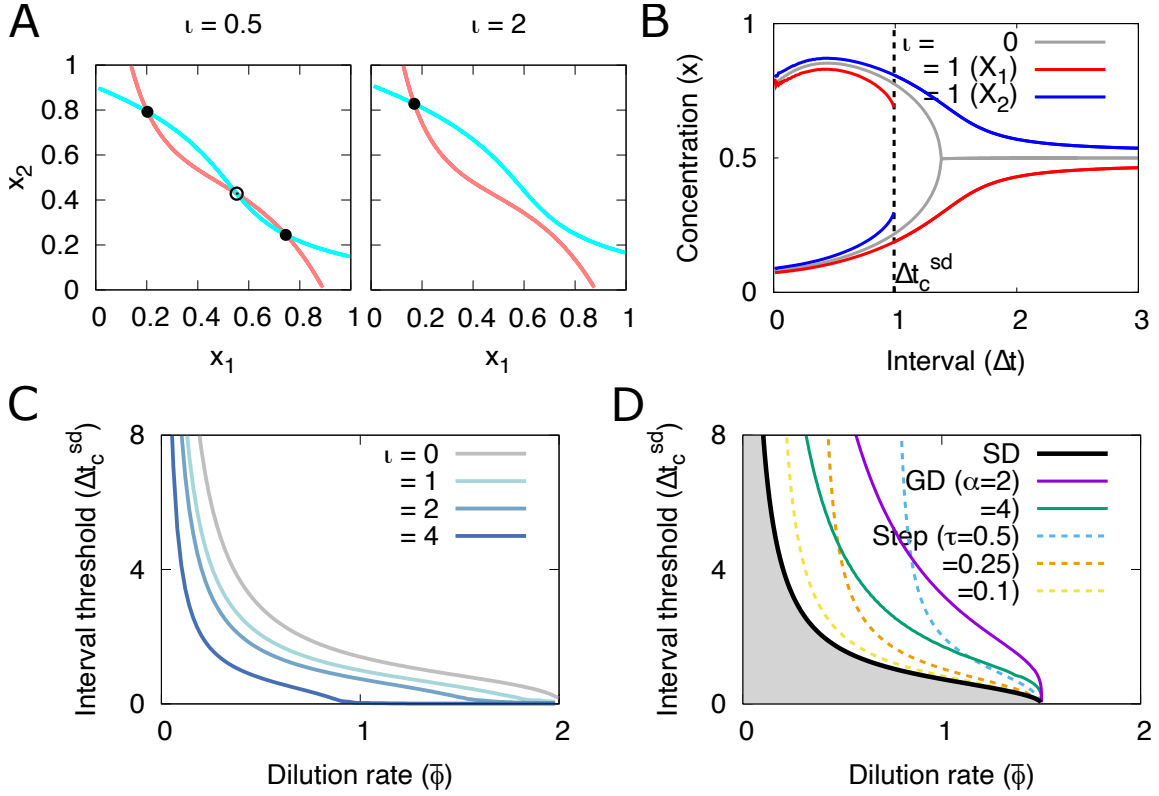


FIG. S4. (A) The red and blue curves represents the nullclines for the composition of the entities  $X_1$  and  $X_2$  at just before the dilution,  $x_1(-0)$  and  $x_2(-0)$ , respectively, in a case with the reproduction rate function are asymmetrical,  $r_i(x)x = \epsilon + \kappa_i x^2$  ( $i = 1, 2$ ) and  $\kappa_1 < \kappa_2$ . The cross points represents the stable/unstable fixed points of concentrations of  $X_1$  and  $X_2$  at just before the dilution,  $x_1^*(-0)$  and  $x_2^*(-0)$ . See Methods and Models for the detail of the drawing of the nullclines. We define  $\kappa_1 = \kappa - \frac{\kappa}{2}$  and  $\kappa_2 = \kappa + \frac{\kappa}{2}$ , and set  $\Delta t = 1$ ,  $\kappa = 8$ ,  $\epsilon = 0.5$ ,  $\bar{\phi} = 1$ , and  $\kappa_2 - \kappa_1 = \nu = 0.5$  (left) and 2 (right). (B) The bifurcation diagram of the concentrations of the entities  $X_1$  and  $X_2$  with a varying period of the dilution cycles  $\Delta t$ . In contrast with the symmetric case (i.e.,  $\nu = 0$ ), the  $X_1$ -dominant state (and thus the bistability) disappears discontinuously at around  $\Delta t_c^{sd} \sim 1.0$ . (C) The dependence of the critical period  $\Delta t_c$  of the cycle on  $\bar{\phi}$ .

$$\frac{d}{dt} \left( \frac{\delta}{\chi} \right) = \frac{1}{\chi^2} \left( \frac{d\delta}{dt} \chi - \frac{d\chi}{dt} \delta \right) = \frac{1}{2} s \chi \left( \frac{\partial r}{\partial x_i} \left( \frac{\chi}{2}, \frac{\chi}{2} \right) - \frac{\partial r}{\partial x_{-i}} \left( \frac{\chi}{2}, \frac{\chi}{2} \right) \right) \frac{\delta}{\chi}. \quad (\text{S8})$$

The integration of  $\frac{d}{dt} \left( \frac{\delta}{\chi} \right) / \left( \frac{\delta}{\chi} \right)$  lead to

$$\begin{aligned} \log \left| \frac{\delta(t)}{\chi(t)} \right| &= \int_0^t \frac{1}{2} s \chi \left( \frac{\partial r}{\partial x_i} \left( \frac{\chi}{2}, \frac{\chi}{2} \right) - \frac{\partial r}{\partial x_{-i}} \left( \frac{\chi}{2}, \frac{\chi}{2} \right) \right) dt + \log \left| \frac{\delta(0)}{\chi(0)} \right| \\ &= \int_{\frac{\chi(0)}{2}}^{\frac{\chi(t)}{2}} \frac{\frac{\partial r}{\partial x_i}(x, x) - \frac{\partial r}{\partial x_{-i}}(x, x)}{r(x, x)} dx + \log \left| \frac{\delta(0)}{\chi(0)} \right|, \end{aligned} \quad (\text{S9})$$

where we used  $\frac{dt}{d\chi} = 1/(sr(\frac{\chi}{2}, \frac{\chi}{2})\chi)$ . Therefore,

$$\frac{\delta(t)}{\chi(t)} = \frac{R_i(\frac{\chi(t)}{2})}{R_i(\frac{\chi(0)}{2})} \frac{R_{-i}(\frac{\chi(0)}{2})}{R_{-i}(\frac{\chi(t)}{2})} \frac{\delta(0)}{\chi(0)}, \quad (\text{S10})$$

where  $R_i(x)$  and  $R_{-i}(x)$  are defined as  $R_i(x) = \exp \left( \int^x \frac{\partial r}{\partial x_i}(x', x')}{r(x', x')} dx' \right)$  and  $R_{-i}(x) = \exp \left( \int^x \frac{\partial r}{\partial x_{-i}}(x', x')}{r(x', x')} dx' \right)$ . Therefore, the sufficient condition for the bistability of the system is

$$\frac{R_i(\frac{\chi(t)}{2})}{R_{-i}(\frac{\chi(t)}{2})} > \frac{R_i(\frac{\chi(0)}{2})}{R_{-i}(\frac{\chi(0)}{2})}. \quad (\text{S11})$$

Here, if we assume that the separation of variables is possible for the reproduction rate function  $r(x_i, x_{-i})$ ,  $r(x_i, x_{-i}) = f(x_i)g(x_{-i})$ ; then,  $R_i(x) = f(x)$  and  $R_{-i}(x) = g(x)$ . Note that, if  $g(x) = 1$ , then the condition Eq. S11 reduced to Eq. 3 in the main text. For example, in a case with the genetic toggle switch model, the above condition is  $\frac{1+(\frac{\chi(\Delta t)}{2})^n}{\frac{\chi(\Delta t)}{2}} > \frac{1+(\frac{\chi(0)}{2})^n}{\frac{\chi(0)}{2}}$ . Thus this model could show the bistability if  $n > 1$ .

#### 4. Robustness to the stochasticity in reaction systems or protocols

##### a. stochasticity in the reaction dynamics and transition between states

If the number of molecules is small (e.g., the reaction dynamics occur inside sufficiently small compartments), stochastic fluctuations are not negligible. Close to the deterministic bifurcation transitions, these fluctuations cause random transitions between states, which destroys the information to be inherited. Thus, the parameter space where the system has heredity is narrower than the deterministic case. However, our main results – the existence of a critical threshold in the dilution interval or the dilution rate and the bistable parameter region for general GD cycles being bounded by that of SD and CSTR – are robust to the addition of stochastic noise in the chemical reaction system.

Previously we discussed the deterministic model, Eq. 1. If the volume of the compartment is small (i.e., the system size) the system, the stochastic fluctuation in the reaction dynamics is non-negligible large [71]. The chemical Langevin equations [71, 72], which is corresponding to Eq. 1 is,

$$\frac{dx_i}{dt} = sr_i(x_i)x_i + \sqrt{sr_i(x_i)V^{-1}}\eta_i(t), \quad (\text{S12})$$

where  $\eta_i$  are i.i.d. Gaussian random variables with the correlation function  $\langle \eta_i(t)\eta_i(t') \rangle = \delta(t - t')$ .  $V$  is the volume of the compartment, and  $V^{-1}$  corresponds to the intensity of noise.

Here, we assume the serial dilution protocol (the volume  $V$  is fixed during one cycle). In contrast with the deterministic case, the transition could occur from  $X_1(X_2)$ -dominant state to the other one in the presence of the stochastic noise (Fig. S5A). We numerically calculate the transition time as in Fig. S6A. We also calculate the transition time in the case that catalytic strength of the entities are asymmetric (see Appendix Sec. S4 in Fig. S6B).

##### b. stochasticity in the dilution protocols

Not only the chemical reaction dynamics but also the dilution protocol, in general, could be stochastic. For example, in the compartment growth and division scenario, the division events could be the stochastic process. The results are also robust to stochasticity in the dilution protocols; for example, if the division time  $\Delta t$  is randomly distributed.

Here, we consider the stochastic serial dilution protocol at which the interval of each dilution event is randomly determined (Fig. S5B). For example, we consider a case that the interval  $\Delta t$  is randomly distributed (e.g., a exponential distribution, whose probability density function  $f(\tau)$  is  $f(\tau) = \lambda \exp(-\frac{\tau}{\lambda})$  where the mean  $\lambda$  is  $\lambda = \langle \Delta t \rangle$ ). We consider the ratio of each dilution  $m$  is constant  $m = e^{\bar{\phi}(\Delta t)}$  (see Fig. S7A for the time course) [73]. In this case, also, there exists the threshold for the time scale  $\langle \Delta t \rangle$  for the system with heredity, although the critical interval  $\langle \Delta t \rangle_c^{sd}$  is less than that for the deterministic case  $\Delta t_c^{sd}$  (see Fig. S7B).

#### 5. Differential reproduction of different chemical compositional states

Finally, we investigate situations where the dilution rates depend on the chemical composition, and the system has different growth rates between the two states. As noted in the introduction, this is, in fact, a crucial property necessary for a population of compartmentalized chemical reaction systems to undergo Darwinian evolution (see Fig. S8).

In such a case, the dilution rate  $\hat{\phi}(t, \mathbf{x}(t))$  is given by  $\hat{\phi}(t, \mathbf{x}(t)) \equiv \frac{dV}{dt}/V$ , such that

$$\int_0^{\Delta t} \hat{\phi}(t, \mathbf{x}_{(i)}^*(t)) = \bar{\phi}_i \Delta t, \quad (\text{S13})$$

where  $i = 1, 2$  and  $\mathbf{x}_{(i)}^*(t)$  represents the steady-state trajectories of  $\mathbf{x}$ , where  $x_i$  is dominant. Here, differential reproduction implies  $\bar{\phi}_1 \neq \bar{\phi}_2$ . Recall that  $m = e^{\bar{\phi} \Delta t}$  is the number of offspring at one generation with interval  $\Delta t$  (main text Sec. A).

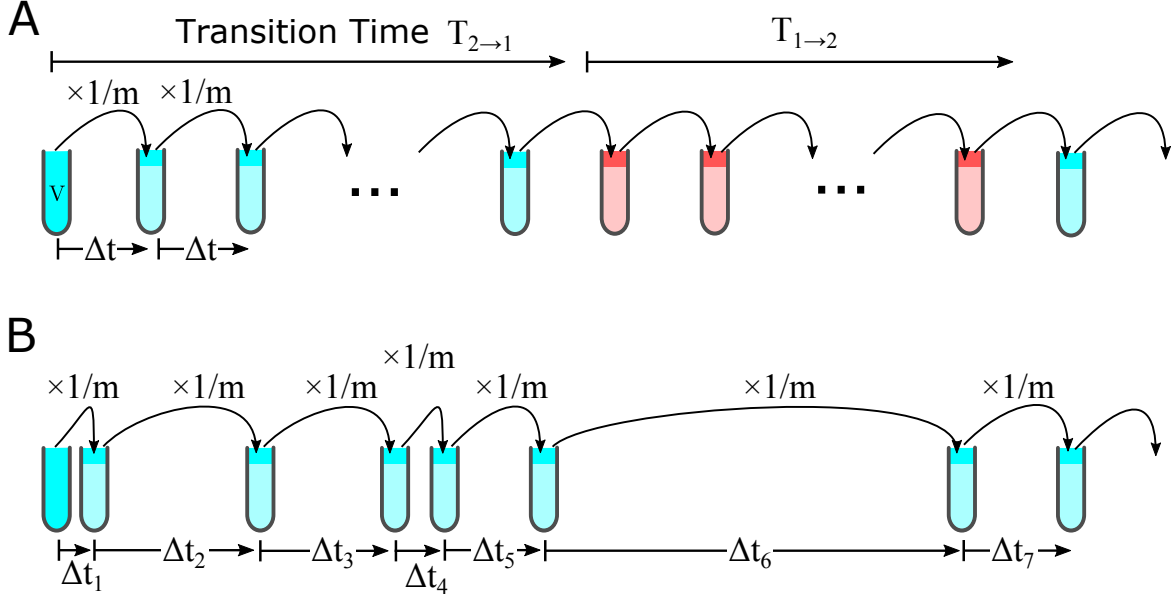


FIG. S5. (A) The stochastic reaction dynamics under the SD. Red and Blue in test tubes (with finite and fixed volume  $V$ ) represent  $X_1$  and  $X_2$ -dominant states, respectively. In contrast with the deterministic case, the fluctuation of concentration causes the transition between states. The (averaged) transition time from  $X_1$  ( $X_2$ )-dominant to  $X_2$  ( $X_1$ )-dominant state is noted as  $T_{1 \rightarrow 2}$  ( $T_{2 \rightarrow 1}$ ). If  $T_{1 \rightarrow 2}$  or  $T_{2 \rightarrow 1}$  are less than the interval  $\Delta t$ , the system has no heredity at all (see Fig. 1 in the main text). (B) The stochastic dilution protocol. The interval at each cycle  $\Delta t_i$  is randomly distributed, and the dilution factor  $m_i$  is  $m = e^{\bar{\phi}(\Delta t)}$ .

As a simple example, we consider the dilution due to the growth of compartments which depends on their components,

$$\hat{\phi}(t, \mathbf{x}(t)) = \phi(t) - \gamma\delta, \quad (\text{S14})$$

where  $\gamma$  is a constant (control parameter),  $\delta = x_1 - x_2$ , and  $\phi(t)$  is the dilution rate independent with the component; here, we choose Eq. 11 in Material and Methods as  $\phi(t)$ , such that  $\int_0^{\Delta t} \phi(t) dt = \bar{\phi}\Delta t$ . Naturally, in this case, the growth rate of the two states are different,  $\bar{\phi}_1 < \bar{\phi}_2$ , if  $\gamma > 0$ . Notably, this dependency of  $\hat{\phi}$  on the composition does not change the critical long-term dilution rate at which the system loses bistability,  $\phi_c$  (Fig. S10A), i.e.,  $\phi_c$  does not depend on  $\gamma$ . Generally, the bistability of the system does not seem to be affected by the asymmetric factor of  $\hat{\phi}$ . We can see this by considering the autocatalytic system is under arbitrary protocols with the dilution rate depending on the chemical composition,

$$\frac{dx_i}{dt} = sr(x_i)x_i - \phi(t, \chi, \delta). \quad (\text{S15})$$

where  $\chi = x_1 + x_2$ ,  $\delta = x_1 - x_2$ . The dependency of  $\phi$  on  $\delta$  is interpreted as differential reproduction between the states. The same calculation as in Appendix Sec. A leads to

$$\frac{d\chi}{dt} = sr\left(\frac{\chi}{2}\right)\chi - \phi(t, \chi, 0)\chi + \mathcal{O}(\delta), \quad \frac{d\delta}{dt} = s\left(r\left(\frac{\chi}{2}\right) + \frac{1}{2}\chi\frac{dr}{d\chi}\left(\frac{\chi}{2}\right)\right)\delta - \phi(t, \chi, 0)\delta + \mathcal{O}(\delta^2), \quad (\text{S16})$$

where  $\chi \gg \delta$  is assumed. Then, the deviation of  $\delta$  in one cycle is calculated as the same as in Appendix Sec. A,

$$\log \left| \frac{\delta(t)}{\chi(t)} \right| = \int_0^t \frac{1}{2} s \frac{dr}{d\chi} \left( \frac{\chi}{2} \right) \chi dt + \log \left| \frac{\delta(0)}{\chi(0)} \right|, \quad (\text{S17})$$

which, notably, does not depend on the asymmetric part of  $\phi(t, \chi, \delta)$ .

Next, we consider a case where  $\phi$  depends on symmetrically  $x_1$  and  $x_2$ , i.e.,  $\hat{\phi}(t, x_1, x_2) = \hat{\phi}(t, x_2, x_1)$ :

$$\hat{\phi}(t, \mathbf{x}(t)) = \phi(t) - \gamma\chi, \quad (\text{S18})$$

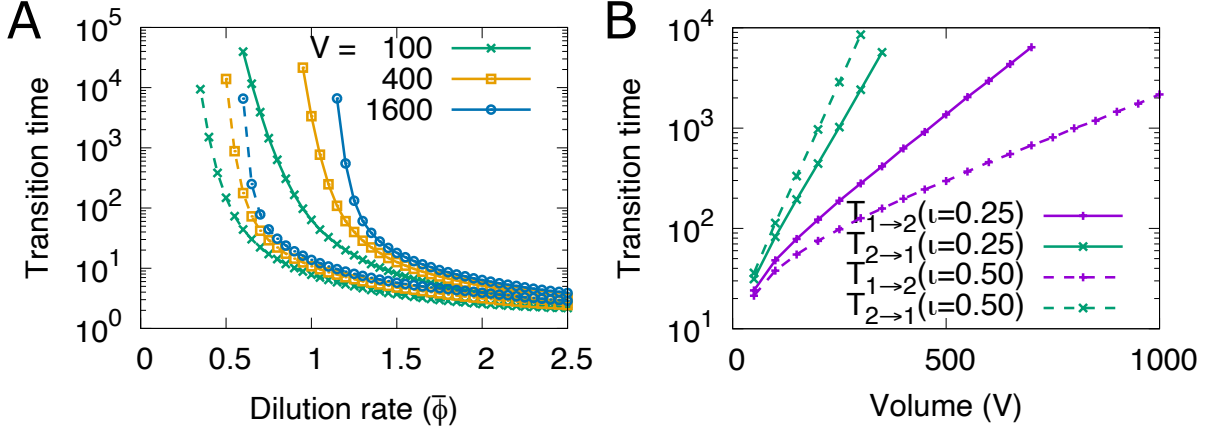


FIG. S6. (A) The transition time from  $X_1$  to  $X_2$ , or the reverse direction,  $T_{1 \rightarrow 2}$  or  $T_{2 \rightarrow 1}$ , varying the dilution rate  $\bar{\phi}$ , under SD protocol. The transition time  $T_{1 \rightarrow 2}$  is calculated as the average of 10000 trials (the time until  $x_2 > x_1$  starting from  $(x_1, x_2) = (s^{tot}, 0)$ ). The lines with different colors represent the difference in the volume  $V$ . Solid lines represent the interval  $\Delta t = 1$ , and dashed ones  $\Delta t = 2$ . We set  $\epsilon = 0.5, \kappa = 8$ , in  $r(x)x = \epsilon + \kappa x^2$ . (B) The transition time between states in the case with asymmetric catalytic strength (from  $X_1$ -dominant to  $X_2$ ,  $T_{1 \rightarrow 2}$  (blue), and the reverse direction (green)). We set  $\iota = 0.25$ , or  $\iota = 0.5$  ( $\kappa_1 = \kappa - \frac{\iota}{2}$  and  $\kappa_2 = \kappa + \frac{\iota}{2}$ ) in the solid or dashed lines, respectively, and  $\Delta t = 1$ .

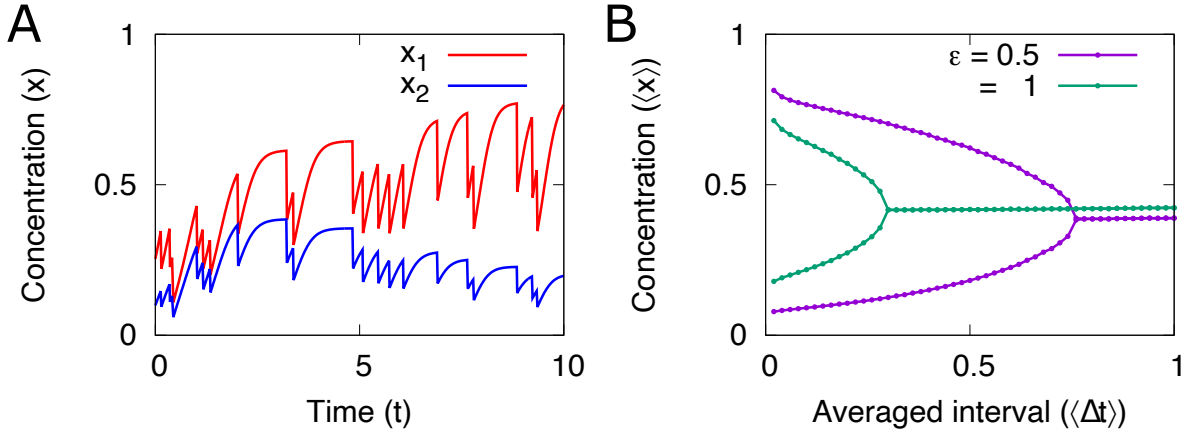


FIG. S7. (A) Time series of  $X_1$  and  $X_2$  in a case with  $r(x)x = \epsilon + \kappa x^2$ . The interval  $\Delta t$  is randomly distributed, while  $m$  is fixed as  $e^{\langle \Delta t \rangle \phi}$ . We set  $\langle \Delta t \rangle = 0.5$ ,  $\epsilon = 0.5$  and  $\kappa = 8$ . (B) The bifurcation diagram of the averaged value of  $x_1$  and  $x_2$  just before the dilutions in the stationary trajectory.

where  $\chi = x_1 + x_2$ , while the catalytic strength of two entities,  $\kappa_1$  and  $\kappa_2$ , are asymmetrical, i.e.,  $\kappa_1 \neq \kappa_2$ , as discussed in Appendix Sec. B2. In this case, also the growth rate is different for different states (Fig. S10).

We also consider a situation where the division interval  $\Delta t$  depends on the composition  $\mathbf{x}$ . For example, we decide whether  $\Delta t$  is equal to  $\Delta t_1$  if  $x_1 > x_2$  at the beginning of cycle, or  $\Delta t_2$  otherwise. Trivially, in this case also, the system has the bistability if  $\Delta t_1$  and  $\Delta t_2$  are below the critical value discussed in the main text Sec. C,  $\Delta t_1, \Delta t_2 < \Delta t_c$ .

Overall, even the case that growth rate  $\phi$  or/and the division interval  $\Delta t$  depend on the chemical composition of the system, we can guarantee the bistability if  $\phi$  at each stationary trajectory,  $\mathbf{x}_{(1)}^*(t)$  and  $\mathbf{x}_{(2)}^*(t)$  satisfies  $\bar{\phi}_1, \bar{\phi}_2 < \phi_c^{sd}$  and  $\Delta t_1, \Delta t_2 < \Delta t_c^{sd}$ .



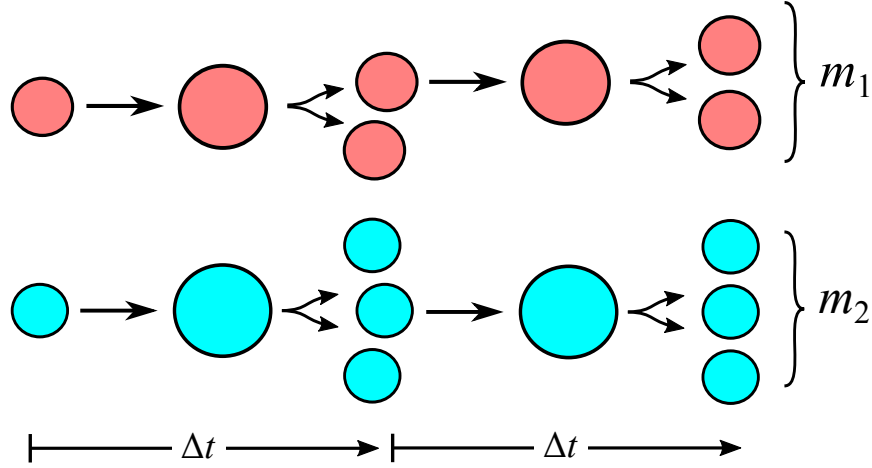


FIG. S8. Schematic diagram for the differential reproduction of compartments. The compartments with the  $X_1$ - and  $X_2$ -dominant states are represented as red and blue circles, respectively. Each compartment grows and produces  $m_1 = e^{\bar{\phi}_1 \Delta t}$  (or  $m_2 = e^{\bar{\phi}_2 \Delta t}$ ) daughters with the equal volumes in the interval  $\Delta t$ . In this figure, the  $X_2$ -dominant compartment grows faster and produces more offspring, i.e.,  $m_2 > m_1$ .

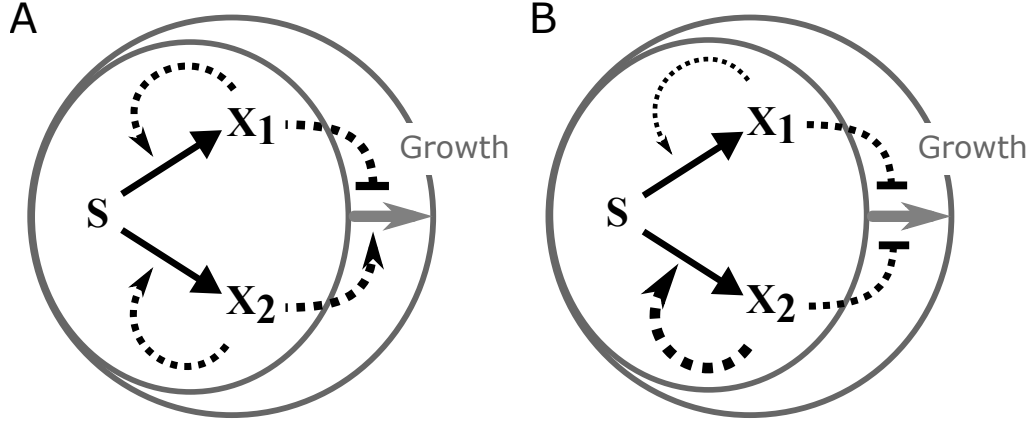


FIG. S9. Schematic diagrams of competing autocatalytic entities encapsulated by a growing compartment. The grey arrow represents the growth of the compartment, which is promoted (dotted arrow) or inhibited (bar-headed dotted arrow) by entities. (A) The entities have symmetric catalytic strength (the same model as Fig. S2A), but affect the compartment growth asymmetrically (see Eq. S14). (B) The entities have asymmetric catalytic strength (the same model as Fig. S2C), but affect the growth symmetrically (see Eq. S18).

### Appendix C: ACS based on *Azoarcus* ribozyme coupled with metabolism

In the case of the system based on *Azoarcus* ribozyme coupled with catabolism/anabolism reaction (Eq. 6 in Sec. II.F in the main text), we drew the same figures as the model (Eq. 1) in Sec. II.B, C and D. These results are qualitatively similar as shown in Fig. S11 and Fig. S12.

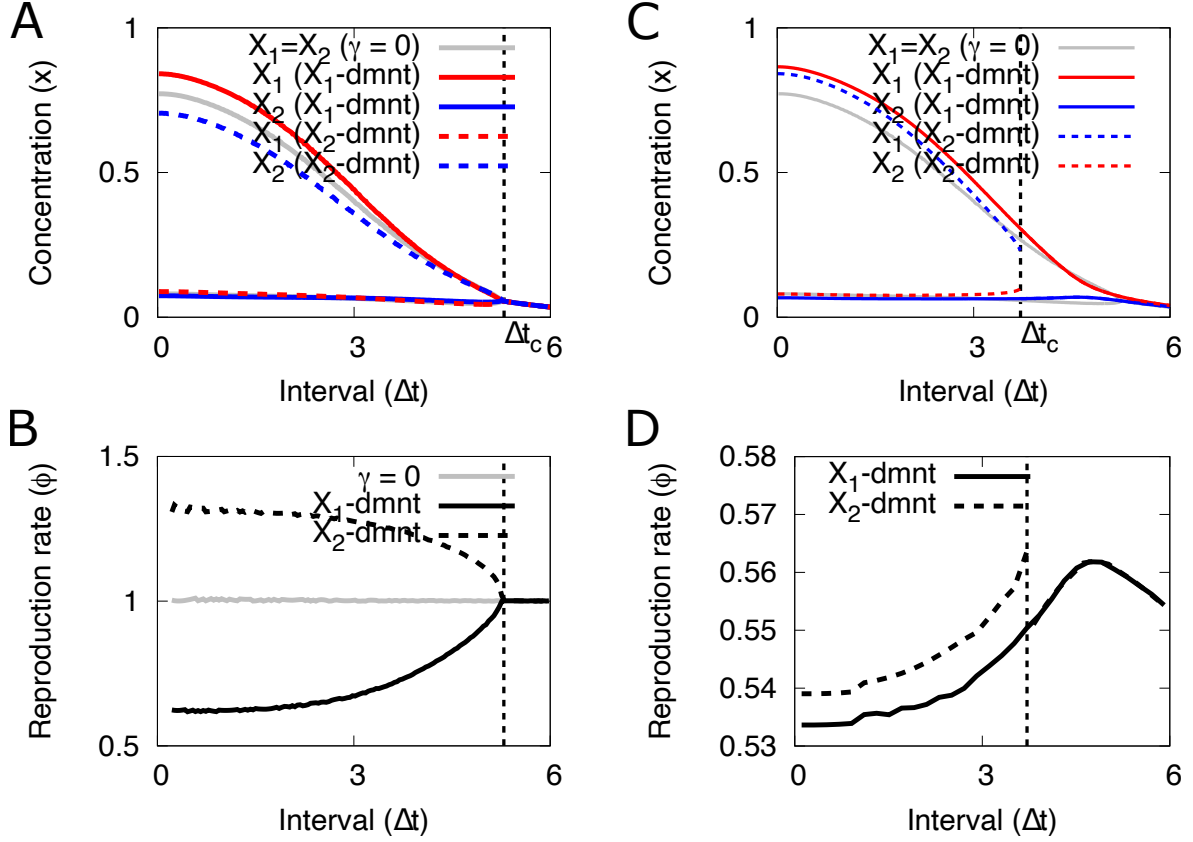


FIG. S10. (A) The bifurcation diagram with a varying cycle interval  $\Delta t$  in a case with  $r(x)x = \epsilon + \kappa x^2$ , the asymmetric dilution rate  $\hat{\phi}(t, \mathbf{x}(t)) = \phi(t) - \gamma\delta$ , where  $\phi(t)$  is given by Eq. 11. The grey curve represents the concentration,  $x_1$  (or  $x_2$ ), at just before dilution in the stationary trajectory when  $\gamma = 0$ , and solid and dashed colored curves represent the concentration when  $\gamma = 1$  in  $X_1$ -dominant and  $X_2$ -dominant states, respectively; the red and blue curves represents  $x_1$  and  $x_2$ , respectively. We set the parameters as  $\kappa = 8$ ,  $\epsilon = 0.5$  and  $\alpha = 2$ . (B) The reproduction rates of the compartment (i.e., the long-term cycle averaged dilution rate),  $\frac{1}{\Delta t} \int_T^{T+\Delta t} \hat{\phi}(t, \mathbf{x}(t)) dt$  as  $T \rightarrow \infty$ , at each compositional state (stationary trajectory  $\{\mathbf{x}(t)\}$ ), varying the interval  $\Delta t$ . The dotted line represents the critical point  $\Delta t_c^{sd}$  which divides the regions where the system has bistability or not. (C) The same bifurcation diagram as (A) in a case with  $r_i(x)x = \epsilon + \kappa_i x^2$  and the symmetric dilution rate  $\hat{\phi}(t, \mathbf{x}(t)) = \phi(t) + \gamma\chi$ . (D) The reproduction rates of the compartment, under the same setup as (B). We set the parameters as  $\iota = -1$ ,  $\kappa = 8$ ,  $\epsilon = 0.5$  and  $\alpha = 2$ .

## Appendix D: Robustness of the results for the system based on *Azoarcus* ribozyme

### 1. In the case with asymmetric catalytic efficiency

A similar relation also appears even when the catalytic activity of two species are different, i.e.,  $\kappa_1 \neq \kappa_2$  (Fig. S14A). Although the bifurcation at which the bistability disappears is discontinuous, it is at the similar  $\Delta t_c$  unless the difference between  $\kappa_1$  and  $\kappa_2$  is not so large Fig. S14B.

### 2. The variation of two-step ACSs with or without heredity

Here, assuming the mass action kinetics, we investigate alternative models with two-step reactions, similar to the model discussed in the main text (Fig. S15A).

Firstly, if we assume the substrate S is consumed in another reaction (see Fig. S15B), the result does not change

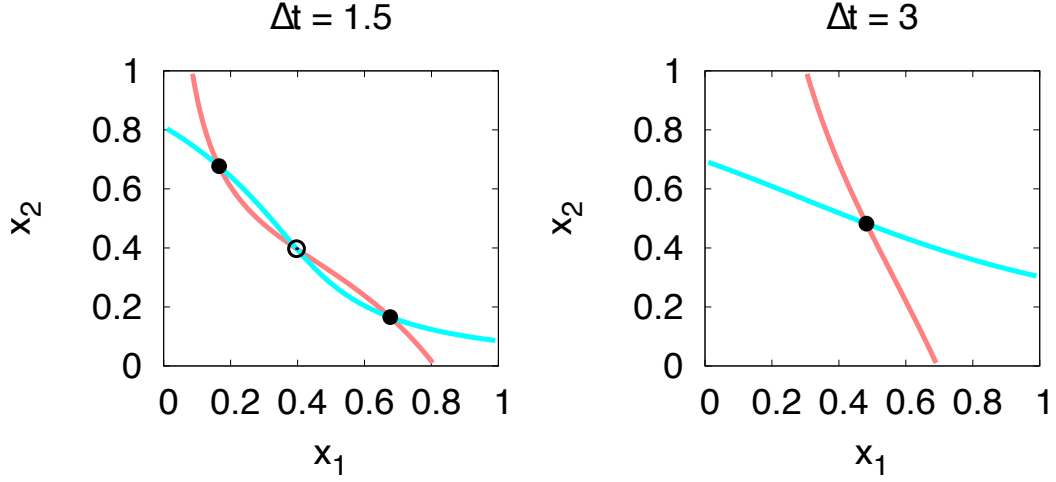


FIG. S11. The red and blue curves represent the nullclines for  $X_1$  and  $X_2$ , respectively, just before dilution. We set  $\Delta t = 1.5, 3$ ,  $\kappa = 2.5$ ,  $\epsilon = 0.25$ ,  $\bar{\phi} = 1$ , and  $b = 0.1$ .

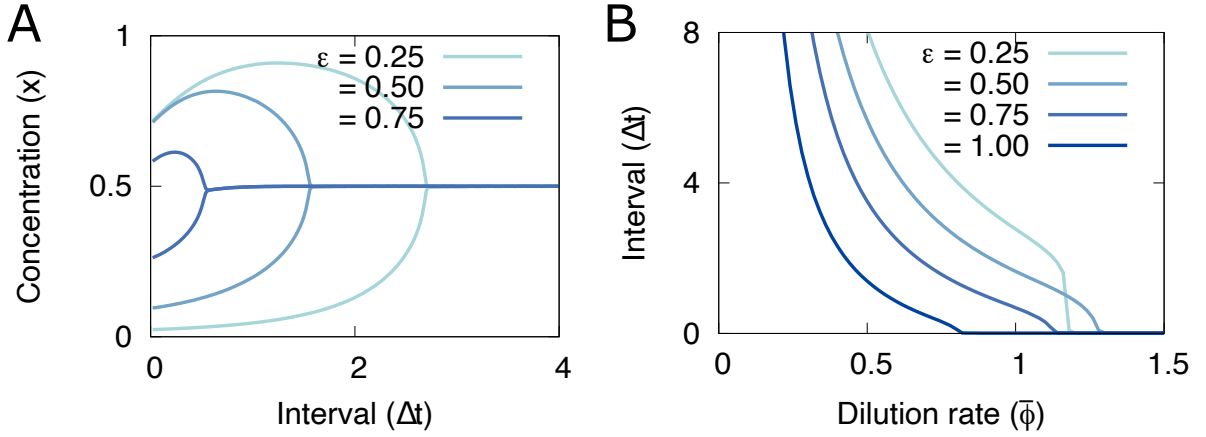


FIG. S12. (A) The bifurcation diagram for the concentration at just before dilution varying the cycle interval  $\Delta t$ . The lines with different colors represent the difference in the background reaction rate  $\epsilon$ . (B) The lines represent the critical point  $\Delta t_c$ , which divides the regions where the system has bistability or not. We set the parameters as  $\kappa = 2.5$  and  $\bar{\phi} = 1$ .

qualitatively; Here, assuming the CSTR condition, we consider the modified rate equations,

$$\frac{dx'_i}{dt} = (\epsilon + \kappa x_i)(s - x'_i) - \bar{\phi} x'_i, \quad \frac{dx_i}{dt} = (\epsilon + \kappa x_i)x'_i - \bar{\phi} x_i, \quad (\text{S1})$$

where  $s^{tot} = s + x'_1 + x'_2 + x_1 + x_2$ .  $X'_1$  and  $X'_2$  are converted from the shared substrate  $S$ , and which are further converted into  $X_1$  and  $X_2$ , respectively.

Then, we consider the dynamics near the steady state, and if we assume  $x'_1$  and  $x'_2$  can be adiabatically eliminated from  $\frac{dx'_i}{dt} = 0$ ,

$$\frac{dx_i}{dt} = \frac{s(\epsilon + \kappa x_i)^2}{\epsilon + \kappa x_i + \bar{\phi}} - \bar{\phi} x_i. \quad (\text{S2})$$

Thus, this rate equation corresponds to Eq. 1 with the reproduction rate function  $xr(x) = \frac{(\epsilon + \kappa x)^2}{\epsilon + \kappa x + \bar{\phi}}$ . Further, in this model also  $X_1$  and  $X_2$  compete for the same substrate  $S$ ; therefore, this model also shows the bistability, if the

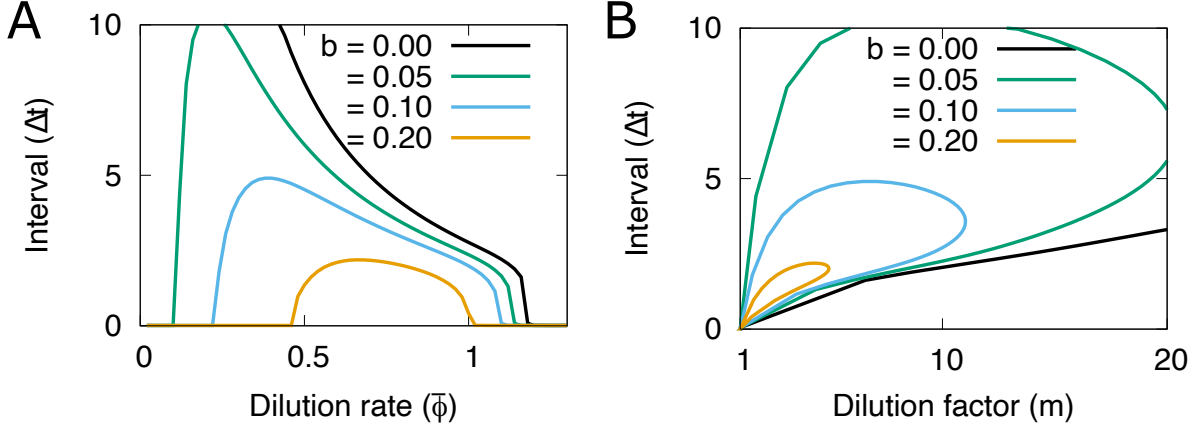


FIG. S13. The parameter region for the system based on *Azoarcus* ribozyme (Eq. 6) with the bistability under SD protocol. The same plot as Fig. 6D in the main text, but its horizontal axis is the dilution factor  $m$ ,  $m = \exp(\bar{\phi}\Delta t)$ , instead of  $\bar{\phi}$ . The lines with different colors represent the boundary between with/without bistability under different backward reaction rates  $b$ . We set  $\epsilon = 0.25$ ,  $\kappa = 2.5$ , and  $b = 0.1$ .

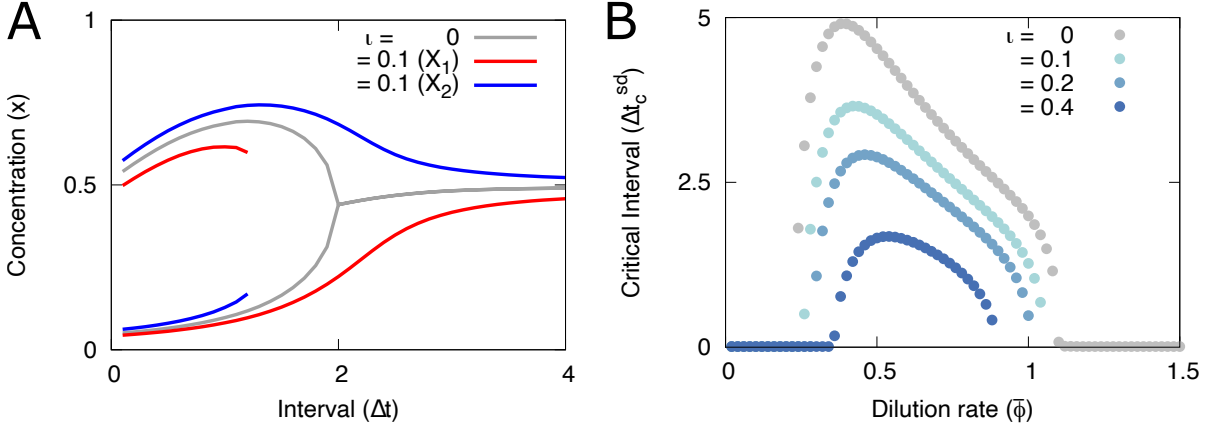


FIG. S14. (A) The concentrations of the species  $X_1$  and  $X_2$  with a varying the period of the dilution cycles  $\Delta t$ , when the catalytic strengths are asymmetric,  $\kappa_1 \neq \kappa_2$ . We set  $\kappa_1 = \kappa - \frac{\iota}{2}$  and  $\kappa_2 = \kappa + \frac{\iota}{2}$ , and  $\kappa_1 - \kappa_2 = \iota = 0.1$ . In contrast with the symmetric case (i.e.,  $\iota = 0$ ), the  $X_2$ -dominant state (and thus the bistability) disappears discontinuously at around  $\Delta t \sim 1.71$ . We set the other parameters as  $\kappa = 2.5$ ,  $\epsilon = 0.25$ ,  $b = 0.1$  and  $\bar{\phi} = 1$ . (B) The dependence of the critical interval  $\Delta t_c^{sd}$  of the cycle on the dilution rate  $\bar{\phi}$  when the catalytic strengths are asymmetric:  $\kappa_1 - \kappa_2 = \iota = 0, 0.05, 0.1$ , and  $0.2$ . We set the other parameters as  $\kappa = 2.5$ ,  $\epsilon = 0.25$ , and  $\bar{\phi} = 1$ .

condition  $\frac{d}{dt}r(\chi^*/2) > 0$  is satisfied, where  $s^*r(\chi^*/2) = \phi$ . (Later, the condition for this reaction system to be bistable under the serial dilution protocol is derived.)

Secondly, for the system show bistability, both of the reactions, from  $S$  to  $X'_1$  and from  $X'_1$  to  $X_1$  have to be catalyzed by  $X_1$ ; for example, we modify the model as the reaction  $S$  to  $X'_1$  is catalyzed by  $X'_1$  instead of  $X_1$  (Fig. S15C). Under the CSTR condition, the rate equations of the model are

$$\frac{dx'_i}{dt} = (\epsilon + \kappa x'_i)(s - x'_i) - \bar{\phi}x'_i, \quad \frac{dx_i}{dt} = (\epsilon + \kappa x_i)x'_i - \bar{\phi}x_i, \quad (\text{S3})$$

where  $s^{tot} = s + x'_1 + x'_2 + x_1 + x_2$ . This system has only one stable fixed point and does not show bistability. This is because,  $X_1$  and  $X_2$  does not compete for the same resource for their replications but  $X'_1$  and  $X'_2$  does. Then, the effective reproduction rate functions for  $X'_1$  and  $X'_2$  do not satisfy the condition for the symmetric state to be unstable.

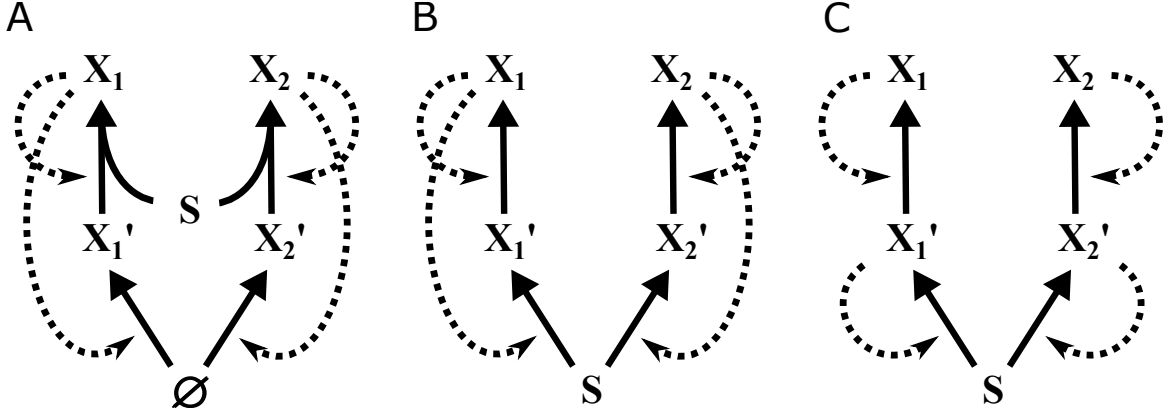


FIG. S15. Schematics of the alternative models for the symmetric competing autocatalytic entities with two reaction steps. Solid arrows represent the reactions, and dotted arrows represent the catalysis. (A) The autocatalytic ribozymes coupled with anabolism and catabolism reactions in the main text Fig. 6B. (B) A similar reaction system with two catalyzed reaction steps, but the substrate  $S$  is consumed to produce  $X_1'$  and  $X_2'$  instead of  $X_1$  and  $X_2$ . (C) Two competing Lotka-Volterra model.

In conclusion, if the mass action kinetics is assumed, for the competing autocatalytic chemical reaction networks sharing the same substrate to have bistability (i.e., the nonlinear reproduction rate function), it is required at least two reaction steps to produce the autocatalytic entities (catalysts), which is catalyzed by the entities themselves.

### 3. derivation of $\Delta t_c^{sd}$ in a case with two-step catalyzed reactions

We further consider the two competing chemical reaction networks with two catalyzed reaction steps in Fig. S15B, under the SD protocol:

$$\frac{dx'_i}{dt} = (s(\{x'_j\}, \{x_j\}, t) - x'_i)r(x_i), \quad \frac{dx_i}{dt} = x'_i r(x_i), \quad (\text{S4})$$

where  $r(x) = \epsilon + \kappa x$ . Here, we define

$$\chi = x_1 + x_2, \quad \chi' = x'_1 + x'_2, \quad \delta = x_1 - x_2, \quad \delta' = x'_1 - x'_2. \quad (\text{S5})$$

The time derivative of the above is derived as

$$\begin{aligned} \frac{d\delta}{dt} &= \frac{1}{2}\delta\chi' \frac{dr}{dx} \left(\frac{\chi}{2}\right) + \delta' r \left(\frac{\chi}{2}\right) && + \mathcal{O}(\delta^2, \delta\delta', \delta'^2), \\ \frac{d\chi}{dt} &= \chi' r \left(\frac{\chi}{2}\right) && + \mathcal{O}(\delta^2, \delta\delta', \delta'^2), \\ \frac{d\delta'}{dt} &= s\delta \frac{dr}{dx} \left(\frac{\chi}{2}\right) - \delta' r \left(\frac{\chi}{2}\right) - \frac{1}{2}\chi' \delta \frac{dr}{dx} \left(\frac{\chi}{2}\right) && + \mathcal{O}(\delta^2, \delta\delta', \delta'^2), \\ \frac{d\chi'}{dt} &= 2sr \left(\frac{\chi}{2}\right) - \chi' r \left(\frac{\chi}{2}\right) && + \mathcal{O}(\delta^2, \delta\delta', \delta'^2), \end{aligned} \quad (\text{S6})$$

where we used  $r(x_i) = r(\frac{\chi}{2}) \pm \frac{\delta}{2} \frac{dr}{dx}(\frac{\chi}{2}) + \mathcal{O}(\delta^2)$ .

To determine the deviation of  $\delta$  in one cycle, we integrate  $\frac{d\delta}{dt}/\delta$ ,

$$\begin{aligned} \int_0^t \frac{d\delta}{\delta} dt &= \frac{1}{2} \int_0^t \chi' \frac{dr}{dx} \left(\frac{\chi}{2}\right) dt + \int_0^t r \left(\frac{\chi}{2}\right) \frac{\delta'}{\delta} dt, \\ &= \int_{\frac{\chi(0)}{2}}^{\frac{\chi(t)}{2}} \frac{dr}{dx} \frac{dx}{r} + \int_{\frac{\chi(0)}{2}}^{\frac{\chi(t)}{2}} \frac{2\delta'}{\chi' \delta} dx, \end{aligned} \quad (\text{S7})$$

where we used the change of the variable  $\frac{dt}{d\chi} = 1/(\chi' r(\frac{\chi}{2}))$ .

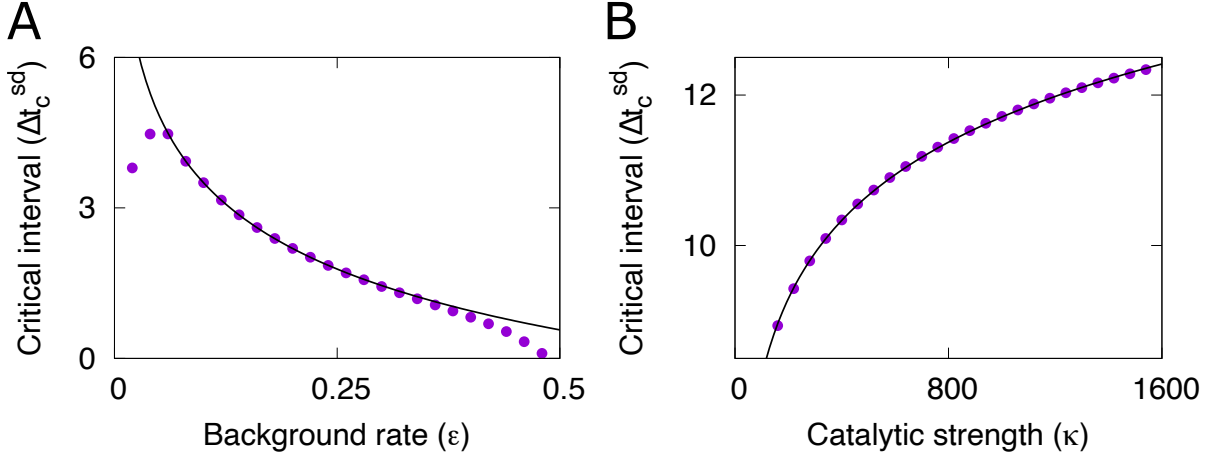


FIG. S16. (A) The solid line represents the critical point  $\Delta t_c$ , which divides the regions where the system has bistability or not. The solid line represents the theoretical line for  $\Delta t_c$  determined by the relation in Eq. S10. (B) The interval threshold  $\Delta t_c$  vs the catalytic efficiency  $\kappa$ , fitted by  $\frac{3}{2} \log(1 + \kappa/2/\epsilon) - C_1$ . We set  $\bar{\phi} = \bar{\sigma} = 1$ .

Here, to calculate Eq. S7, we have to estimate  $\delta'/\chi'$  in the second integral in Eq. S7. If we assume in the second term, in the dominant part of the integrand,  $\delta'/\chi'$  has the scaling relation  $\delta'/\chi' \sim \mathcal{O}(1)$ ,

$$\frac{\delta'}{\chi'} \approx \frac{\frac{d\delta'}{dt}}{\frac{d\chi'}{dt}} = \frac{1}{2} \frac{dr}{dx} \delta - \frac{\delta'}{2s - \chi'} \approx \frac{1}{2} \frac{dr}{dx} \delta, \quad (\text{S8})$$

where we used  $\frac{d}{dt}(\frac{\delta'}{\chi'}) = 0$  in the first approximation, and in the second approximation, we assumed  $s \gg \chi'$ . We substitute this to the above equation,

$$\log \left| \frac{\delta(t)}{\delta(0)} \right| \approx 2 \log \left| \frac{r(\frac{\chi(t)}{2})}{r(\frac{\chi(0)}{2})} \right|. \quad (\text{S9})$$

The threshold of  $\Delta t$  for the symmetric (i.e.,  $\delta = 0$ ) trajectory to be unstable is,

$$\Delta t_c^{sd} = \frac{2}{\bar{\phi}} \log \left( 1 + \frac{\kappa s^{tot}}{2\epsilon} \right) - C_0, \quad (\text{S10})$$

where  $C_0$  is a constant value, which is determined by numerically as  $C_0 \sim 3.6$  (see Fig. S16A).

While we use the asymptotic relation  $\frac{\delta'}{\chi'^2} \sim \mathcal{O}(1)$  as  $t$  becomes large. Then,

$$\frac{\delta'}{\chi'} \approx \frac{1}{2} \frac{\frac{d\delta'}{dt}}{\frac{d\chi'}{dt}} \approx \frac{1}{4} \frac{dr}{dx} \delta, \quad (\text{S11})$$

where  $\frac{d}{dt}(\frac{\delta'}{\chi'^2}) = 0$  in the first approximation, and  $s \gg \chi'$  in the second as like before. Thus,

$$\log \left| \frac{\delta(t)}{\delta(0)} \right| \approx \frac{3}{2} \log \left| \frac{r(\frac{\chi(t)}{2})}{r(\frac{\chi(0)}{2})} \right|, \quad (\text{S12})$$

and then

$$\Delta t_c^{sd} = \frac{3}{2\bar{\phi}} \log \left( 1 + \frac{\kappa s^{tot}}{2\epsilon} \right) - C_1, \quad (\text{S13})$$

where  $C_1$  is numerically determined as  $C_1 \sim 0.477$  (see Fig. S16B).